GEOCHEMISTRY AND U/PB ZIRCON GEOCHRONOLOGY OF THE VIRGIN ISLANDS BATHOLITH, BRITISH VIRGIN ISLANDS

Kevin Lee Schrecengost

A thesis submitted to the faculty of the University of North Carolina at Chapel Hill in partial fulfillment of the requirements for the degree of Master of Science in the Department of Geological Sciences.

Chapel Hill
2010

Approved by:

Allen F. Glazner

Drew S. Coleman

Lara Wagner

ABSTRACT

Kevin Lee Schrecengost: Geochemistry and U/Pb zircon geochronology of the Virgin Islands batholith, British Virgin Islands
(Under the direction of Allen F. Glazner)

The Virgin Islands batholith is a series of mid-crustal granitic rocks in an oceanic island arc. Here I present new whole-rock major- and trace-element compositions, Sr, Pb, and Nd isotopic data, zircon Hf-O isotopic data, and U/Pb zircon geochronology for the batholith.

Zircon geochronology indicates that the batholith was assembled over ≥13 m.y. between 43.6 and 30.6 Ma with the emplacement of at least four discrete suites. The batholith is marked by spatio-temporal and geochemical patterns. Initial $^{87}Sr/^{86}Sr$, $\varepsilon_{Nd}(t)$, zircon $\varepsilon_{Hf}(t)$, and zircon $\delta^{18}O$ suggest that the batholith evolved from mantle-derived melts with limited incorporation of isotopically evolved crustal components.

Evidence from the batholith suggests that oceanic island arcs produce nascent continental crust that evolves toward average continental compositions. This immature crust is likely a precursor to the production of continental crust that has yet to undergo further differentiation. This nascent stage provides an important step in continental crust production.

ACKNOWLEDGEMENTS

I would like to thank a great number of people, more than I am likely to remember in writing this acknowledgment. I am indebted to the knowledge, skill, and generosity of so many. Firstly, I would like to thank my committee: Allen Glazner, Drew Coleman, and Lara Wagner; for providing guidance throughout this journey along with J. J. W. Rogers who provided a majority of the funding and initial idea to revisit the granitic rocks of the Virgin Islands batholith. I would also like to thank Sigma Xi and the UNC Martin Fund for additional funding. I would like to acknowledge Jesse Davis, Mike Tappa, Ryan Mills, Mike Lester, and Ayumi Shimokawa with all of their help in and out of the lab, constant willingness to lend an ear, and without whom this manuscript would be a mere shadow of itself. I would also like to give a big thanks to the all of the graduate and undergraduate students that I had the pleasure to meet along the way; you made it a pleasure and that says a lot. Mostly, I would like to thank my friends and family; my mother, Rebecca; my father, Richard; and my brother, Brian for their unconditional love, unwavering support, and insistent reminders of what it is all about.

TABLE OF CONTENTS

LIST OF TABLES

Table

LIST OF FIGURES

Figure

LIST OF ABBREVIATIONS

CA	Calc-alkaline association
BVI	British Virgin Islands
$\varepsilon Nd_{(t)}$	Initial epsilon neodymium
HREE	Heavy rare earth element
ID-TIMS	Isotope dilution thermal ionization mass spectrometry
ICP-MS	Inductively coupled plasma mass spectrometry
LA-ICP-MS	Laser ablation inductively coupled plasma mass spectrometry
LREE	Light rare earth element
MSWD	Mean square of the weighted deviate
REE	Rare earth element
PIA	Primitive island arc association
$^{87}Sr/^{86}Sr_{(i)}$	Initial ^{87} Strontium / ^{86} Strontium
TIMS	Thermal ionization mass spectrometry
TTG	Tonalite-trondjhemite-granodiorite
VIB	Virgin Islands batholith

CHAPTER 1

Introduction

The formation of continental crust and the origin of granitic magmatism, a key building block of continental crust, remain fundamental problems in geology (e.g. Rudnick, 1995; Petford et al., 2000; Brophy, 2008). The continental crust is consistently estimated to have an andesitic bulk composition (e.g. Taylor and McLennan, 1995; Rudnick, 1995; Wedepohl, 1995). Crustal growth models generally describe the accretion of oceanic island arcs of intermediate compositions as the predominant process by which the continents grow (Taylor, 1966; Condie, 1990; Rudnick, 1995; Condie and Chomiak, 1996). However, oceanic island arcs are dominated by mafic volcanism, whereas intermediate and felsic magmatism characterize the volcanic and plutonic products at continental margins (Rudnick, 1995; Jagoutz et al., 2009).

Granitic magmatism is generally associated with the subduction of oceanic lithosphere beneath continental lithosphere, allowing for significant magmatic differentiation through fractional crystallization, partial melting, and hybridization with the continental crust (Hildreth and Moorbath, 1988; Pitcher, 1997). However, mid-crustal exposures of oceanic island arcs (e.g. Stork, 1984; Donnelly and Rogers, 1980; Greene et al., 2006; Jagoutz et al., 2009) have been found to contain a significant component of granitic material that is not typically associated with subduction at oceanic island arcs (Rudnick, 1995). Exposures of these mid-crustal plutonic rocks, including the Virgin Islands batholith, provide insight into

the production and character of granitic magmatism in oceanic island arcs and the maturation of nascent continental crust.

Helsley (1960, 1971) and Longshore (1965) provided early descriptions of the Virgin Islands batholith, a collection of felsic plutonic rocks largely consisting of tonalite and granodiorite. The batholith is located throughout the British Virgin Islands at the eastern edge of the Greater Antilles, along the border of the Caribbean-North American plate (Fig. 1; Byrne et al., 1985). The Puerto Rico Trench, to the north, and the Muertos Trench, to the south, border the platform, which is separated from the Lesser Antilles by the Anegada Fault to the southeast (Byrne et al., 1985).

Tectonic reconstructions of the Caribbean indicate that the Greater Antilles are the remnants of a long-lived oceanic island arc dating to the Cretaceous (Pindell and Barrett, 1990; Pindell et al., 2006; Pindell and Kennan, 2009). Erosion of the islands of the Greater Antilles has exposed a number of mid-crustal plutonic rocks that record the intrusive history of the arc. Many of the intrusive bodies of the Greater Antilles have been studied in detail (e.g. Donnelly and Rogers, 1978; 1980; Donnelly et al., 1990; Lewis & Draper, 1990), but geochemical studies of the Virgin Islands batholith are limited (e.g. Smith et al., 1998; Lidiak and Jolly, 1998a; Frost et al., 1998). This study contributes new U-Pb zircon geochronology; major-, trace-, and rare earth element data; Nd, Sr, and Pb isotopic data; and zircon Hf and O isotopic data.

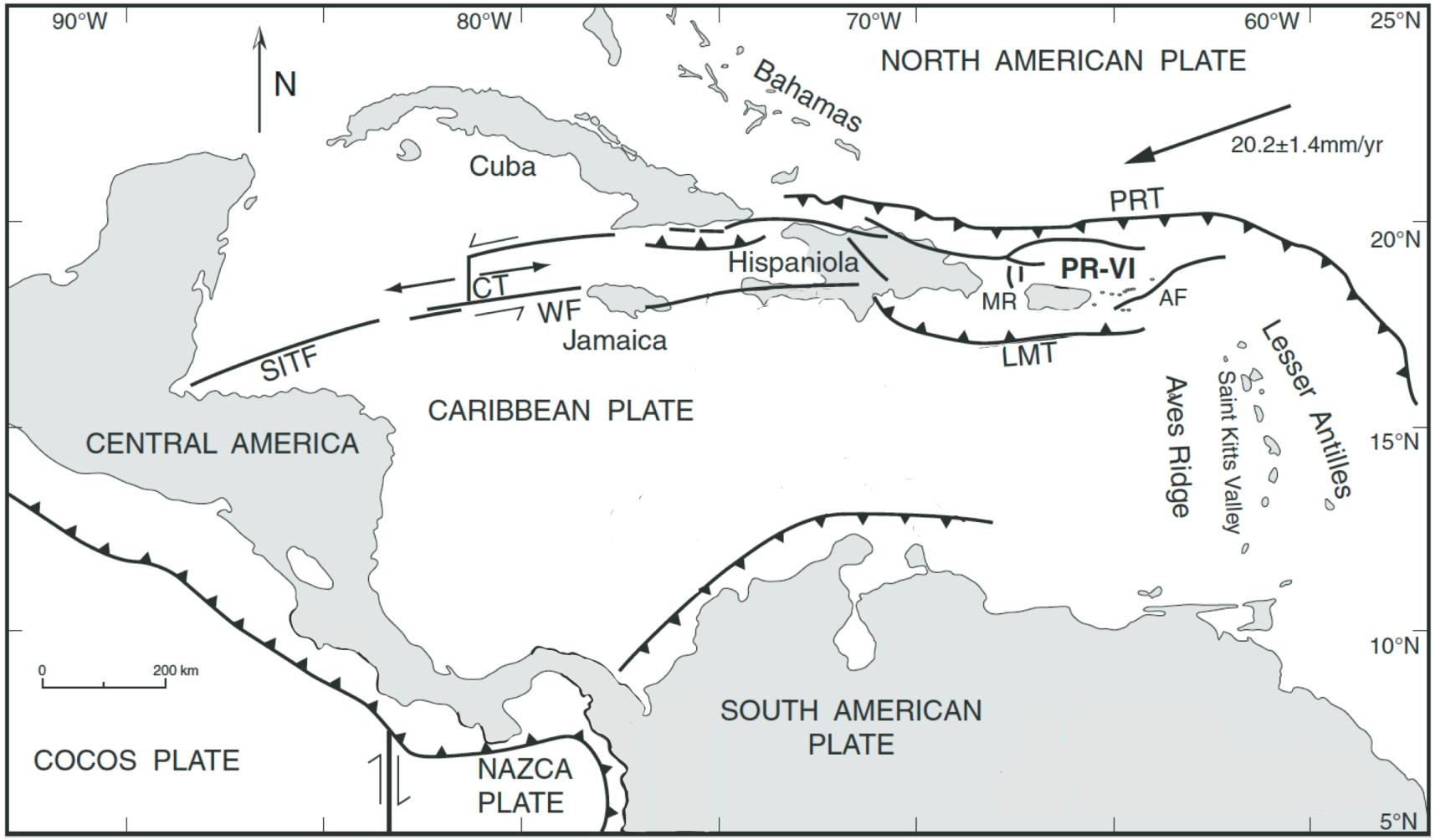

Figure 1: Map of the Caribbean region modified from Jolly et al., 2008, showing structural elements of the North American and Caribbean plates (solid lines are fault zones; teeth indicate polarity of subduction). North American plate vector indicates the motion of the Atlantic basin with respect to a stable Caribbean (Jansma et al., 2000). AF-Anegada Fault; CT-Cayman Trough spreading center; LMT-Los Muertos Trench; MR-Mona rift; PRT-Puerto Rico Trench; PR-VI-Puerto Rico-Virgin Islands platform; SITF-Swan Island Transform Fault; WF-Walton Fault.

Chapter 2

Background

The Greater Antilles are located along the northern boundary of the Caribbean plate where they adjoin the Bahamas platform of the North American plate (Fig. 1). The islands of the Greater Antilles are the products of arc magmatism that began in the Early Cretaceous and continued into the Oligocene. This magmatism owes its origin to subduction between the proto-Caribbean plate and the North American plate (e.g. Donnelly et al., 1990; Lewis and Draper, 1990; Kerr et al., 1999; Jolly et al., 2008). The plate tectonic dynamics of these interactions are unclear and remain heavily debated (e.g. Jolly et al., 2008; James, 2009; Pindell and Kennan, 2009). Current views of Caribbean tectonics suggest that the Caribbean plate originated in the Pacific as part of the Jurassic Farallon plate, requiring migration of the proto-Caribbean plate eastward during the opening of the Atlantic Ocean and separation of Africa from North and South America (Fig. 2; Pindell and Barrett, 1990; Pindell et al., 2006; Pindell and Kennan, 2009). Eastward migration of the proto-Caribbean plate resulted in subduction of oceanic lithosphere in ocean-ocean convergence zones and early island arc development, although the polarity of this early subduction is unclear (e.g. Pindell et al., 2006; Jolly et al., 2008; Pindell and Kennan, 2009). A number of arc polarity reversals of varying scale

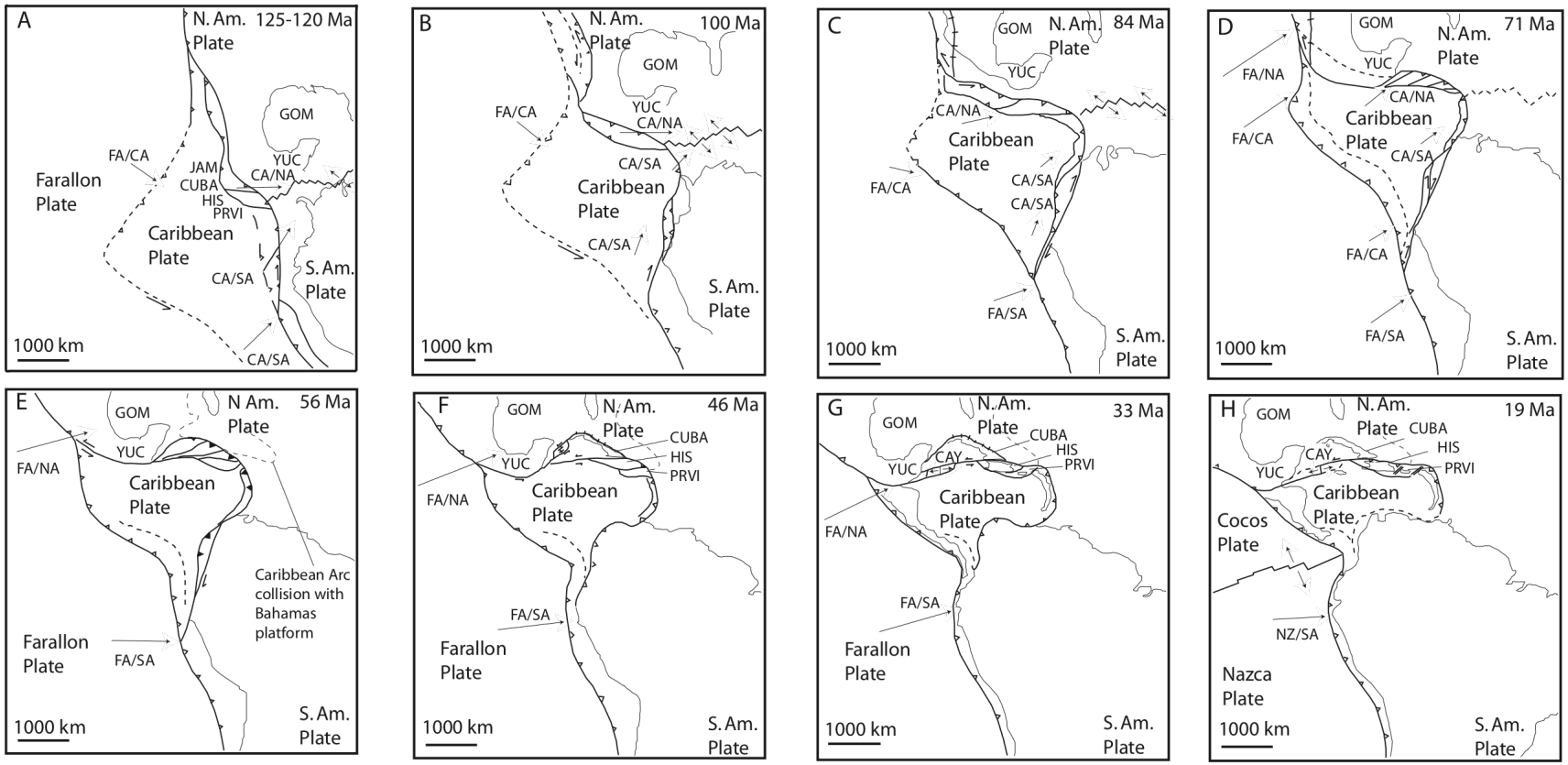

Figure 2: Summary of the tectonic history of the Caribbean plate after Pindell and Kennan (2009). Relative plate motions are with respect to an Indo-Atlantic hot spot reference. A) 125-120 Ma, plate boundaries show relative positions after initiation of SW-dipping subduction beneath the Caribbean Arc. B) 100 Ma, relative motion of the Caribbean to North America is to the east. Eastward migration of transpressive terranes is occurring along the northern and southern edge of the Caribbean. C) 84 Ma, onset of oblique subduction along the southern Farallon-Caribbean boundary. D) 71 Ma, spreading between North and South America ends. E) 56 Ma, oblique intra-arc basins begin opening as the Caribbean spreads eastward. The northern Caribbean Arc begins colliding with the Bahamas platform. F) 46 Ma, northward drift of the Caribbean has stopped. The collision of Cuba translates Caribbean-North America relative motion along the Cayman Trough. G) 33 Ma, Caribbean-North American Plate boundary begin to take its present form. Sinistral transtension begins to dominate the northern Caribbean Plate boundary. H) 19 Ma, subduction along the Greater Antilles has been shut off. PRVI-Puerto Rico-Virgin Islands platform, HIS-Hispaniola, JAM-Jamaica, YUC-Yucatán, GOM-Gulf of Mexico, FA-Farallon, CA-Caribbean, NA-North America, SA-South America, NZ-Nazca.

ranging from the Cretaceous to early Oligocene have been proposed (e.g. Draper et al., 1996; Jolly et al., 1998b; Jolly et al., 2008; Pindell and Kennan, 2009). However, the subduction of oceanic crust from the Atlantic Ocean beneath the arc toward the south and east dominated the subduction history of the Caribbean (Fig. 2; Pindell and Kennan, 2009).

Much of the magmatism associated with the Greater Antilles occurred during the Cretaceous, but magmatism in the eastern Greater Antilles, including the Virgin Islands, continued into the Oligocene (Donnelly et al., 1990; Jolly et al., 1998). Collision of the Greater Antilles arc with the Bahamas platform caused cessation of arc magmatism, with Cuba colliding during the Paleocene-Eocene (Pindell and Barrett, 1990) and Hispaniola during the Eocene-Oligocene (Joyce, 1991). This collision progressively shifted the subduction direction from north-south to east-west, causing a transition from perpendicular to oblique subduction beneath the Puerto Rico-Virgin Islands platform (Fig. 2; Pindell and Kennan, 2009; Smith et al., 1998). Ongoing collision continued the transition to sinistral transtension along the Puerto Rico trench and the opening of the Cayman trough (Rosencrantz and Sclater, 1987). Transtension along this boundary resulted in the concentration of magmatic centers along the northern boundary, counterclockwise rotation of the Puerto Rico and Virgin Islands platform by approximately 25°, and isolation from the main subduction zone during the Miocene (Fig. 2, Reid et al., 1991; Jolly et al., 1998b).

The Puerto Rico-Virgin Islands platform represents the easternmost section of the Greater Antilles. Magmatism on this platform ranges in age from 120 Ma in Puerto Rico to 24 Ma in the Virgin Islands (Smith et al., 1998). Stratigraphy in the Virgin Islands records volcanic and depositional activity since the Late Cretaceous that is punctuated by several unconformities and the intrusion of the Virgin Islands batholith (Helsley, 1960; 1971). The

Cretaceous Water Island Formation is a series of basalt, dacite, and rhyolite volcanic rocks that mark the beginning of arc development in the Virgin Islands (Helsley, 1971). The Water Island Formation is unconformably overlain by andesitic pyroclastic rocks of the Late Cretaceous and Eocene (Helsley, 1971). The dip of these formations varies systematically, south to north, from 50°S (overturned) to 15°N (Helsley, 1971). The Virgin Islands batholith has a total area of approximately 250 km^2 based on inferred underwater extensions and the extent of metamorphic aureoles (Helsley, 1960). The batholith crops out on the islands of Virgin Gorda, Tortola, Little and Great Camanoe, Fallen Jerusalem, Scrub, Cooper, Salt, Beef, and Peter, a total land area of about 35 km^2 (Fig. 3; Helsley, 1960; 1971; Longshore, 1965). K-Ar and Ar-Ar total gas ages of mineral separates from the batholith range from approximately 60 to 24 Ma (Cox et al., 1977; Kessler and Sutter, 1979; Vila et al., 1986; Smith et al., 1998). Helsley (1960, 1971) and Longshore (1965) proposed that the batholith was emplaced during a single magmatic event as a shallow sill-like body. Emplacement of the batholith corresponded to the tectonic transition from perpendicular to oblique subduction in the Eocene to Oligocene, sinistral transtension in the Miocene, and finally migration of the arc to the southeast creating the Lesser Antilles (Fig. 2; Jolly et al., 1998b; Smith et al., 1998). The exposed Virgin Islands batholith comprises approximately 65% tonalite, 25% granodiorite, and 10% gabbro (Longshore, 1965); these rocks are similar to other felsic intrusions in the eastern Greater Antilles (Donnelly and Rogers, 1978, 1980; Lidiak and Jolly, 1996; Smith et al., 1998). Several studies have provided extensive geochemical work on these felsic intrusions but relatively little data exist on the geochemistry of the Virgin Islands batholith beyond major element geochemistry and limited trace-element and isotopic analyses (e.g. Lidiak and Jolly, 1996; Frost et al., 1998; Smith et al., 1998).

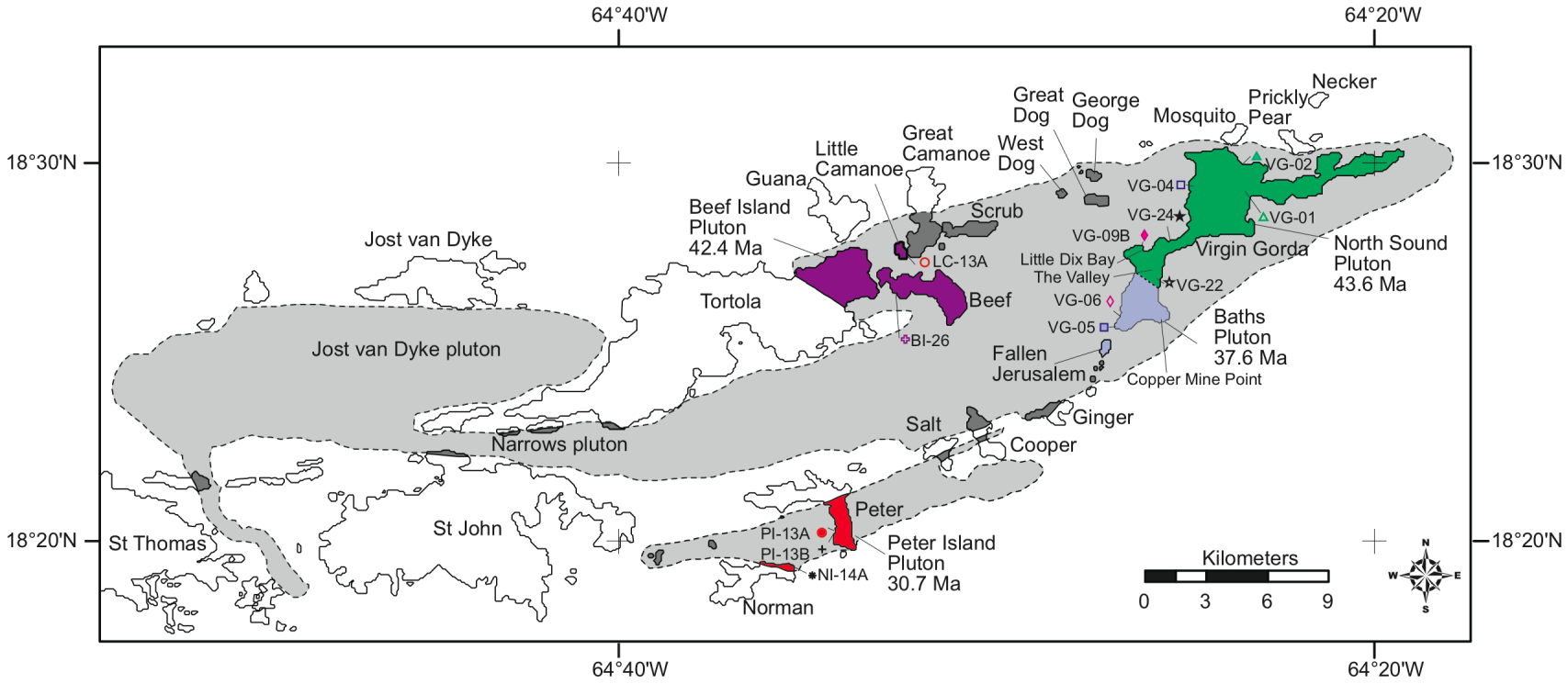

Figure 3: Map of the Virgin Islands batholith and its under water extent modified from Helsley, 1971. Map of plutons within the Virgin Islands batholith, including location and age of geochemical samples.

Magma series throughout the Greater Antilles have been segregated into two groups, the primitive island arc series and the calc-alkaline series (Donnelly and Rogers, 1980). The primitive island arc series is analogous to the island arc tholeiite series in modern arcs (Hastie, 2009) and precedes the appearance of the calc-alkaline series where it occurs in the Greater Antilles (Donnelly and Rogers, 1980). The primitive island arc series has low REE, Th, U, Rb, K, and Ba concentrations and flat REE patterns across the full range of silica values (Donnelly and Rogers, 1980; Hastie, 2009), whereas the calc-alkaline series is enriched in incompatible trace elements and radiogenic isotope ratios (Hastie, 2009). In the Virgin Islands, the primitive island arc series is represented by the Cretaceous Water Island Formation and the Virgin Islands batholith are associated with the calc-alkaline series (Donnelly and Rogers, 1980; Lidiak and Jolly, 1996).

Why there should be granitic magmatism in the northeastern Caribbean is unclear. Granitic bodies developing within oceanic crust though not unheard of, are unusual (Greene et al., 2006; Jagoutz et al., 2009). The crust beneath the Greater Antilles is relatively thick, 7-10 km on average, and reaches up to 30-35 km (Case et al., 1990). This crustal thickness may arise from the presence of granitic material throughout the Greater Antilles; however, this thick crust may provide a mechanism by which granitic magmatism is produced (Annen et al., 2006). The directionality of the cause-effect relationship between crustal thickness and granitic magmatism in the Greater Antilles is uncertain.

Smith et al. (1998) proposed that high geothermal gradients throughout the Upper Cretaceous and Lower Tertiary in the Puerto Rico and Virgin Islands platform allowed for partial melting of early island arc materials in the lower crust during transpressive downbuckling of the arc, creating granitic melts that were emplaced in the upper crust along

shear zones in Puerto Rico. This transpressive regime ended by the Eocene requiring a different emplacement mechanism for the Virgin Islands batholith (Smith et al., 1998). During the Eocene-Oligocene, the direction of subduction transitioned from perpendicular to oblique convergence that created room for the intrusion of partial melts into the upper crust (Smith et al. 1998).

Chapter 3

Methods

Sampling

Sample collection and was conducted in May 2008. Exposure of the batholith is largely limited to shoreline outcrops with limited access, but several construction sites and road cuts allowed for fresh exposure on Virgin Gorda, where sampling was focused. Additional sampling occurred on the islands of Peter, Beef, the Dogs, Little Camanoe, Norman, Cooper, and Tortola. Hand samples and geochemical samples (typically 1 kg of fresh rock chips) were taken at each collection site. Geochronology samples (typically 2 kg of rock chips) were gathered at seven locations. All samples were examined in thin section under a petrographic microscope and named based on IUGS classification (Appendix A).

Geochemistry

To characterize petrologic, geochemical, and geographic diversity within the batholith thirteen samples were selected for geochemical analysis based on lack of obvious alteration. Geochemical samples were ground to powders using a steel jaw crusher and ceramic shatterbox. Whole-rock powders were sent to Activation Laboratories Ltd. for major and trace element analysis. Samples were processed using lithium metaborate/tetraborate fusion. Major-elements and Ba, Sr, Y, Zr, Sc, Be, and V were analyzed using inductively couple plasma atomic emission spectroscopy and the remaining trace elements were analyzed by inductively coupled plasma-mass spectrometry.

Whole-rock Sr, Nd, and Pb isotopic ratios were determined using a VG Sector 54 thermal ionization mass spectrometer at the University of North Carolina at Chapel Hill. Sample powders were dissolved in hydrofluoric acid and cations were separated using standard column chemistry. Strontium was separated using Sr-spec resin. Anion exchange chromatography was used to separate Pb. Neodymium was isolated in two stages. The first stage used Re-spec for bulk separation of REE and the second separated Sm from Nd using methylactic acid chemistry (Devine, 1969). Samples were loaded on single Re filaments. Strontium and Pb were analyzed as metals, and Nd was analyzed as an oxide. Lead ratios were corrected for fractionation by 0.12% per amu based on internal lab standards. Whole-rock Pb ratios are not age corrected due to Pb concentrations below detection limits in all but one sample. Analytical precision of Sr, 0.000000008 (2σ), is based upon replicate analyses of the standard NBS987. Analytical precision of Nd, 0.512098 ± 0.000018 (2σ), is based upon replicate analyses of the standard JNdi (Tanaka et al., 2000). Strontium ratios were normalized to $^{86}Sr/^{88}Sr = 0.1194$. Neodymium ratios were normalized to $^{146}Nd/^{144}Nd = 0.7219$. Samples were not spiked for isotope dilution; concentrations of Rb, Sr, Sm, Nd, and Pb were obtained from geochemical analysis at Activation Laboratories Ltd. $^{87}Sr/^{86}Sr_i$ and $\varepsilon_{Nd}(t)$ indicate values corrected to the age of the sample as reported in Table 3. Epsilon Nd values were calculated using $^{143}Nd/^{144}Nd(CHUR) = 0.512638$ and $^{147}Sm/^{144}Nd(CHUR) = 0.1967$.

Zircon mineral separates from VG-01 (North Sound), BI-26 (Beef Island), VG-05 and VG-06 (Baths), and PI-13A (Peter Island) were analyzed by Charlotte Allen at the Australia National University using laser ablation inductively couple plasma mass spectrometry for Hf and O isotopes (Table 5). Hafnium isotopes were corrected for age using results of this study

and laser ablation inductively coupled plasma mass spectrometry zircon ages of the same sample. Analytical errors are reported as one standard deviation of the mean. Oxygen isotopes have relatively high quoted uncertainty due to high background readings and smoothing (C. Allen, personal communication, 2010).

Geochronology

Four samples from the batholith were selected for zircon U/Pb geochronology. Samples were crushed using a steel jaw crusher and a disc mill. Zircon was separated by density, using a water table and heavy liquids. A Frantz magnetic separator was used for final separation, using the magnetic property of the grains. Zircons were then selected under a binocular microscope for size, morphology, and the absence of cracks and inclusions. Zircons from each sample contain few inclusions and lack apparent cores or rims reflecting inheritance. Selected grains were thermally annealed for 72 hours at 900°C (Mattinson, 2005) and chemically abraded in 29 M HF acid at 180°C for 12 hours to remove areas exposed to Pb loss (modified from Mundil et al., 2004). Zircons were removed from chemical abrasion and washed with HNO_3 and H_2O to remove HF acid from the surface of the zircon grains. Zircon grains were grouped based on size and morphology and separated into separate fractions for analysis. Fractions were dissolved in 29 M HF acid and spiked using a ^{205}Pb-^{233}U-^{236}U tracer (Krogh, 1973; Parrish and Krogh, 1987). Aliquots were passed through anion exchange chromatography to isolate U and Pb. Isotopic analyses were run on the VG Sector 54 thermal ionization mass spectrometer at the University of North Carolina at Chapel Hill. Uranium was loaded on single Re filaments in graphite and H_3PO_4 and run as a metal. Lead was loaded in silica gel on single Re filaments and run as a metal. Uranium and lead were analyzed using a single-collector Daly ion-counting system. Isotopic data were reduced

using Tripoli™ and standard errors are reported at 2σ confidence intervals. Ages were calculated using the PbMacDat-2 program by D.S. Coleman using algorithms from Ludwig (1990, 1989) and Isoplot v. 3.00 (Ludwig, 2003). Decay constants used are $^{238}U = 1.55125 \times 10^{-10}\ a^{-1}$ and $^{235}U = 9.8485 \times 10^{-10}\ a^{-1}$ (Steiger and Jäger, 1977).

Chapter 4

Results

Field relationships and sampling

The Virgin Islands batholith encompasses a large area (~ 250 km^2) of felsic plutonic rocks on the northeastern corner of the Caribbean plate. The lack of three-dimensional exposure within the batholith complicates efforts to determine the orientation and structure of the batholith. Field observations suggest that the batholith is compositionally heterogeneous with a number of small bodies of gabbro, quartz diorite, tonalite, and granodiorite. The batholith has been interpreted to represent a single Eocene magmatic episode, but includes at least four suites of differing age and character. Here we describe new field observations and provide names for these bodies (Fig. 3). The bodies are named and grouped by their compositions and geographic distribution, but we have not attempted new mapping and use these groupings only to facilitate discussion.

The North Sound suite of northeastern Virgin Gorda is a fine-grained, heterogeneous, felsic body. The suite includes subunits of quartz diorite, tonalite, and granodiorite. Pervasive mafic enclaves appear in granodiorite members on the southwestern side of the suite, near the Valley.

On western Virgin Gorda, near Little Dix Bay, a subunit of heterogeneous hornblende gabbro displays local modal layering, textural coarsening, and orbicular structures. Textural and geochemical evidence suggest this gabbro is a cumulate. The gabbro

may represent the southernmost extent of the North Sound suite or the easternmost extent of the Beef Island suite based on geochemical relationships.

The Beef Island suite crops out on Beef, Scrub, Tortola, Great Camanoe, and Little Camanoe Islands. The suite is composed of granodiorite on Beef Island and a fine-grained tonalite on the Camanoe islands. Orthogonal, steeply dipping, north- and east-striking mafic dikes cut the tonalite on Little Camanoe.

The Baths suite, a relatively homogenous hornblende granodiorite with local hornblende foliation, crops out in southern Virgin Gorda and on Fallen Jerusalem Island. A north-striking fault zone near Copper Mine Point cuts the Baths suite and is on strike with a shear zone that cuts through the isthmus east of Little Dix Bay.

Sheets of tonalite, diorite, and basalt with interleaved metamorphic wall-rock screens characterize the Peter Island suite on Peter and Norman Islands. These screens strike roughly north with near vertical dip, and range in thickness from 1 to 4 m. Tonalite sheets on Norman Island exhibit internal contacts with chilled margins and include granodiorite xenoliths resembling the Baths suite, suggesting that the Peter Island suite may cut the Baths suite.

Major- and trace-element geochemistry

Components of the Virgin Islands batholith range from gabbro to granodiorite (Table 1; Figs. 4-7). Silica content is bimodal, ranging from 43-53 and 62-76 wt% with K_2O ranging from 0.09-2.14 wt%. The highest silica concentrations, VG-02 and LC-12B, are from the North Sound and Beef Island suite, respectively. The low silica end-member, VG-09B, is a cumulate located at Little Dix Bay Samples from the Peter Island suite stand out from the main geochemical trends with more enriched Ba, Sr, and Cr and less enriched in Zr, Sc (Fig. 5).

Table 1: Whole-rock major-element concentrations (wt.%)

	VG-01	VG-02	VG-04A	VG-05	VG-06	VG-09B	LC-12B	PI-13A	PI-13B	NI-14A	VG-22	VG-24	BI-26
SiO_2	52.88	72.58	68.26	68.92	65.21	43.31	76.64	62.55	45.03	63.92	63.90	50.87	63.95
TiO_2	0.971	0.360	0.465	0.322	0.416	0.070	0.271	0.306	0.658	0.350	0.497	0.946	0.535
Al_2O_3	20.63	13.04	14.56	15.18	15.92	23.62	11.54	15.67	16.44	16.92	15.60	18.31	15.05
Fe_2O_3(T)	6.70	3.18	4.80	3.84	5.18	7.07	2.91	3.49	11.41	4.11	5.76	10.82	6.33
MnO	0.129	0.053	0.094	0.105	0.135	0.122	0.014	0.100	0.305	0.103	0.123	0.172	0.128
MgO	2.64	0.61	1.49	1.42	2.05	8.78	0.12	2.08	8.13	1.96	2.36	4.38	2.40
CaO	10.85	2.83	4.61	3.99	5.45	14.98	1.87	4.78	11.82	5.75	5.72	10.24	5.64
Na_2O	3.47	4.09	3.95	3.34	3.33	0.71	4.43	3.72	1.28	4.01	3.05	2.81	3.15
K_2O	0.14	1.33	0.95	2.14	1.38	0.09	0.75	1.57	0.53	1.16	1.69	0.32	1.45
P_2O_5	0.25	0.07	0.08	0.10	0.13	0.01	0.06	0.10	0.09	0.14	0.09	0.14	0.07
LOI	0.690	1.020	0.360	0.530	0.410	1.200	0.630	3.900	2.810	0.980	0.590	0.630	0.550
Total	99.36	99.15	99.63	99.88	99.61	99.97	99.23	98.26	98.50	99.42	99.37	99.64	99.24

Table 1: Whole-rock trace-element concentrations (ppm)

	VG-01	VG-02	VG-04A	VG-05	VG-06	VG-09B	LC-12B	PI-13A	PI-13B	NI-14A	VG-22	VG-24	BI-26
Sc	29	14	16	9	11	28	12	10	49	10	20	34	24
Be	1	<1	<1	1	<1	<1	1	1	1	1	<1	1	<1
V	217	34	96	61	89	57	12	80	331	89	129	351	152
Cr	<20	<20	<20	<20	<20	110	<20	50	100	30	<20	40	<20
Co	7	2	8	8	10	43	2	9	36	9	12	26	13
Ni	<20	<20	<20	<20	<20	50	<20	<20	<20	<20	<20	<20	<20
Cu	<10	<10	<10	30	100	20	<10	50	20	30	10	200	30
Zn	70	40	50	50	60	40	30	60	90	40	50	80	60
Ga	20	14	15	14	16	12	13	17	14	17	14	17	14
Ge	1.4	1.5	1.8	1.6	1.4	1	1.5	1	1.6	1.4	1.4	1.4	1.6
As	<5	<5	<5	18	<5	<5	<5	<5	<5	<5	<5	<5	<5
Rb	<1	12	23	57	32	2	8	36	9	25	38	6	29
Sr	262	146	170	212	258	194	100	528	232	643	195	272	153
Y	23.4	39.1	32	13	15.5	1.5	53.1	9.1	12.3	8.9	27.2	15.8	31
Zr	64	176	123	82	129	2	210	64	33	56	105	66	144
Nb	1.4	2.2	1.8	2.1	1.8	0.4	2.1	2.3	0.7	2.2	1.9	1.6	1.5
Mo	<2	<2	<2	<2	<2	<2	<2	<2	<2	<2	<2	<2	<2
Ag	<0.5	<0.5	<0.5	<0.5	<0.5	<0.5	<0.5	<0.5	<0.5	<0.5	0.5	<0.5	<0.5
In	<0.1	<0.1	<0.1	<0.1	<0.1	<0.1	0.2	<0.1	<0.1	<0.1	<0.1	<0.1	<0.1
Sn	4	11	7	10	11	<1	69	3	3	17	3	3	6
Sb	<0.2	<0.2	<0.2	1.4	<0.2	0.5	<0.2	<0.2	0.4	<0.2	<0.2	<0.2	0.6
Cs	<0.1	0.2	1.1	2.1	1.1	0.1	0.1	0.8	0.3	0.7	0.9	0.2	1
Ba	48	445	212	449	324	32	260	823	96	743	378	88	237

Table 1: (cont.) Whole-rock trace-element concentrations (ppm)

	VG-01	VG-02	VG-04A	VG-05	VG-06	VG-09B	LC-12B	PI-13A	PI-13B	NI-14A	VG-22	VG-24	BI-26
La	4.25	7.54	8.73	9.36	7.13	0.25	6.55	6.78	3.24	7.39	7.86	4.98	8.02
Ce	8.63	15.5	18.8	17.5	14.4	0.43	16.6	12	6.75	13.4	17.2	10.3	17.4
Pr	1.51	2.46	2.83	2.19	2.1	0.07	3.11	1.69	1.16	1.88	2.71	1.66	2.67
Nd	7.74	11.3	12	8.02	7.97	0.44	15.2	6.28	5.6	7.08	11.8	7.18	11.6
Sm	2.41	3.21	3.2	1.84	2.02	0.16	4.53	1.47	1.59	1.59	3.17	1.92	3.13
Eu	0.908	0.925	0.909	0.611	0.688	0.118	0.854	0.512	0.591	0.576	0.785	0.766	0.773
Gd	3.44	4.43	4.14	1.91	2.31	0.22	6.41	1.64	2.02	1.61	3.93	2.45	4.13
Tb	0.58	0.8	0.7	0.32	0.39	0.04	1.18	0.24	0.34	0.24	0.66	0.4	0.71
Dy	3.64	5.38	4.68	1.98	2.38	0.27	7.83	1.46	2.08	1.41	4.28	2.53	4.57
Ho	0.82	1.26	1.07	0.43	0.52	0.06	1.78	0.3	0.45	0.29	0.94	0.55	1.03
Er	2.6	4.18	3.45	1.44	1.68	0.16	5.9	0.96	1.43	0.93	3.05	1.79	3.37
Tm	0.387	0.653	0.524	0.23	0.26	0.023	0.914	0.144	0.211	0.14	0.467	0.272	0.516
Yb	2.4	4.23	3.42	1.53	1.73	0.15	5.86	0.92	1.27	0.89	3.01	1.76	3.38
Lu	0.36	0.705	0.55	0.251	0.291	0.024	0.917	0.154	0.184	0.148	0.48	0.266	0.538
Hf	1.8	5.1	3.6	2.7	3.5	<0.1	6.3	1.8	1	1.7	3.1	1.9	4
Ta	0.06	0.13	0.12	0.23	0.13	<0.01	0.12	0.16	0.02	0.13	0.11	0.1	0.1
W	1.5	1	1.6	5	1	1.1	1.2	1.1	1	1.2	1	1.4	1.1
Tl	<0.05	0.26	0.42	0.3	0.33	<0.05	0.09	0.4	0.16	0.19	0.33	0.1	0.4
Pb	<5	<5	<5	18	<5	<5	<5	<5	<5	<5	<5	<5	<5
Bi	<0.1	0.1	<0.1	<0.1	0.1	<0.1	0.2	<0.1	0.1	0.2	0.5	<0.1	<0.1
Th	0.61	2.65	1.87	3.65	1.86	<0.05	1.79	1.45	0.26	1.11	1.62	0.77	2.39
U	0.19	1.32	0.77	0.94	0.65	0.08	0.83	1.01	0.1	0.64	0.84	0.33	1.03

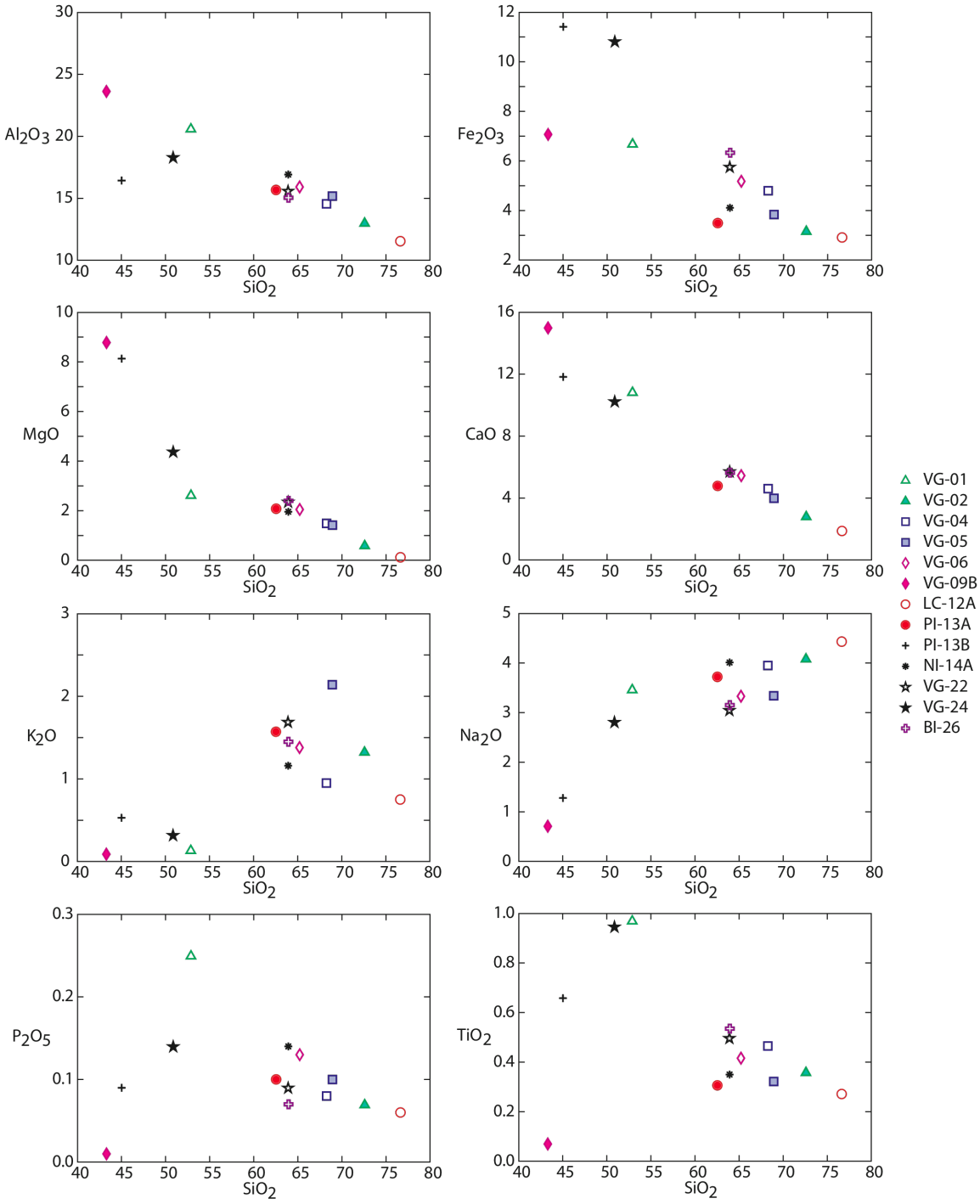

Figure 1: Major-element variations compared with SiO_2 for the Virgin Islands batholth. Major-elements in weight percent.

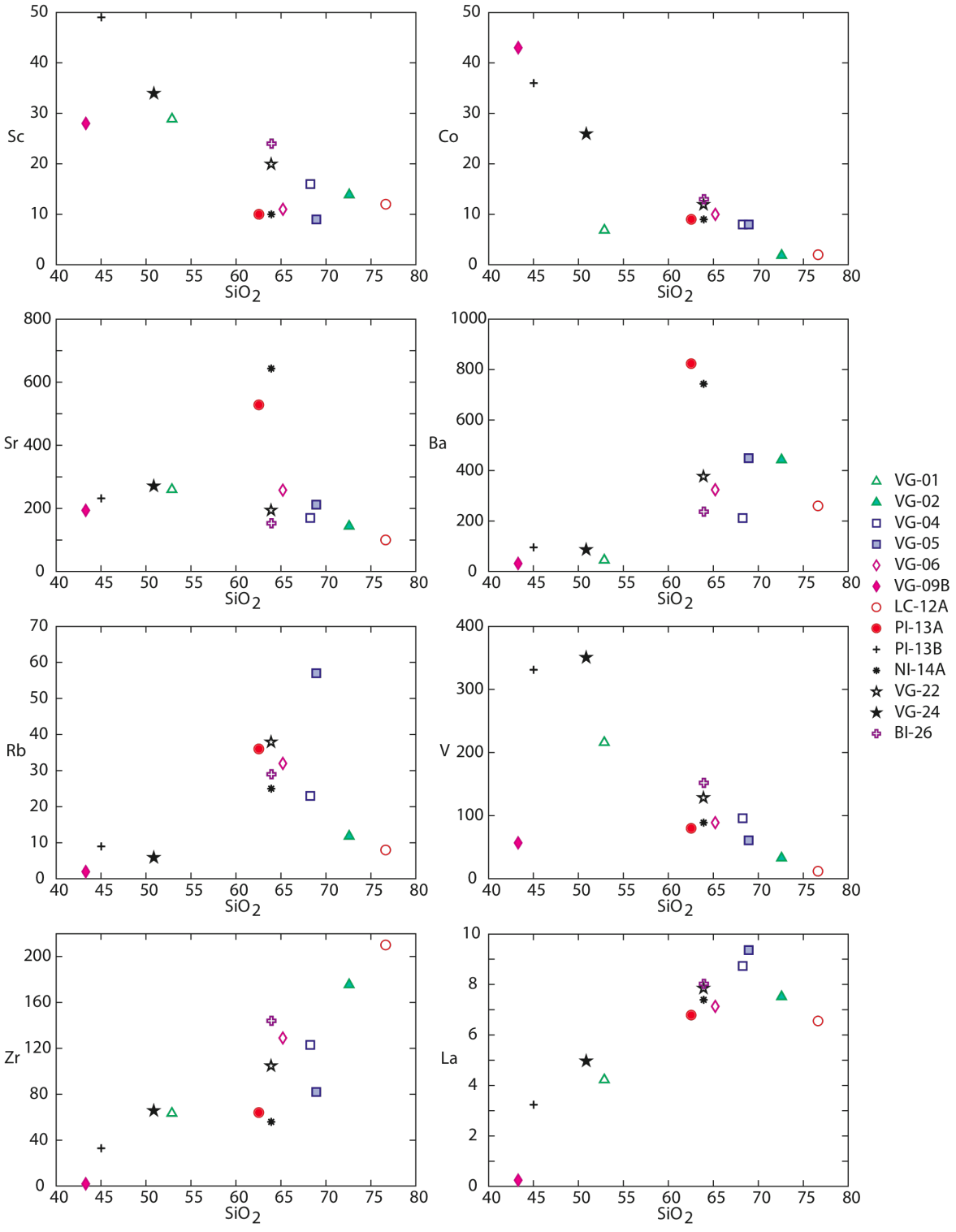

Figure 2: Trace-element variations with SiO_2 for the Virgin Islands batholith. Major-elements in weight percent, trace elements in parts per million.

Rare-earth element (REE) concentrations normalized to chondrite show significant variation throughout the batholith (Fig. 6). Four distinct patterns are identifiable as follows: positive Eu anomalies (Eu enrichment), negative Eu anomalies (Eu depletion), flat, and concave-up (light REE enriched and heavy REE depleted). A hornblende gabbro from the southwestern edge of the North Sound suite at Little Dix Bay, with 42 wt% SiO_2, is the only sample with a positive Eu anomaly. Granodiorites and tonalites from the North Sound and Beef Island suites exhibit negative Eu anomalies. Samples with negative Eu anomalies exhibit a wide range in heavy REE enrichment. Flat REE patterns only occur in samples with SiO_2 less than 55 wt%. The granodiorite and tonalite of the Baths and Peter Island suites to the south display concave-up patterns. Concave-up patterns show a wide range in heavy REE enrichment, similar to samples with negative Eu anomalies.

Multi-element diagrams normalized to primitive mantle (Fig. 7; Sun and McDonough, 1989) show that the felsic bodies of the batholith are relatively depleted in Nb, Ta, P, and Ti. The North Sound and Beef Island suites exhibit steeper troughs at Nb, Ta, P, and Ti relative to those of the Baths and Peter Island suites. The Baths and Peter Islands suites exhibit peaks at Sr not seen in samples from the North Sound and Beef Island suites. One sample from the Baths has a peak at Pb; values for the remaining samples are below the detection limit.

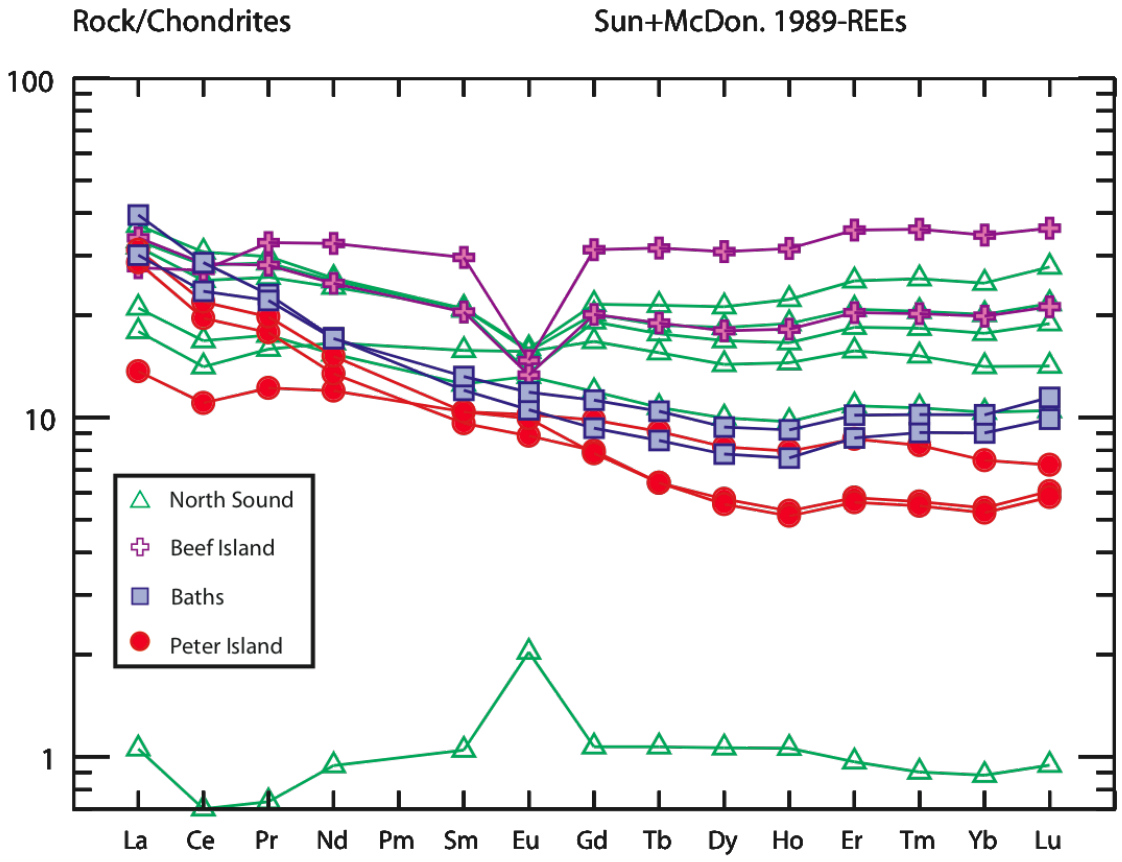

Figure 3: Chondrite-normalized rare earth element patterns for plutons of the Virgin Islands batholith. (Chondrite normalizing factors from Sun and McDonough, 1989).

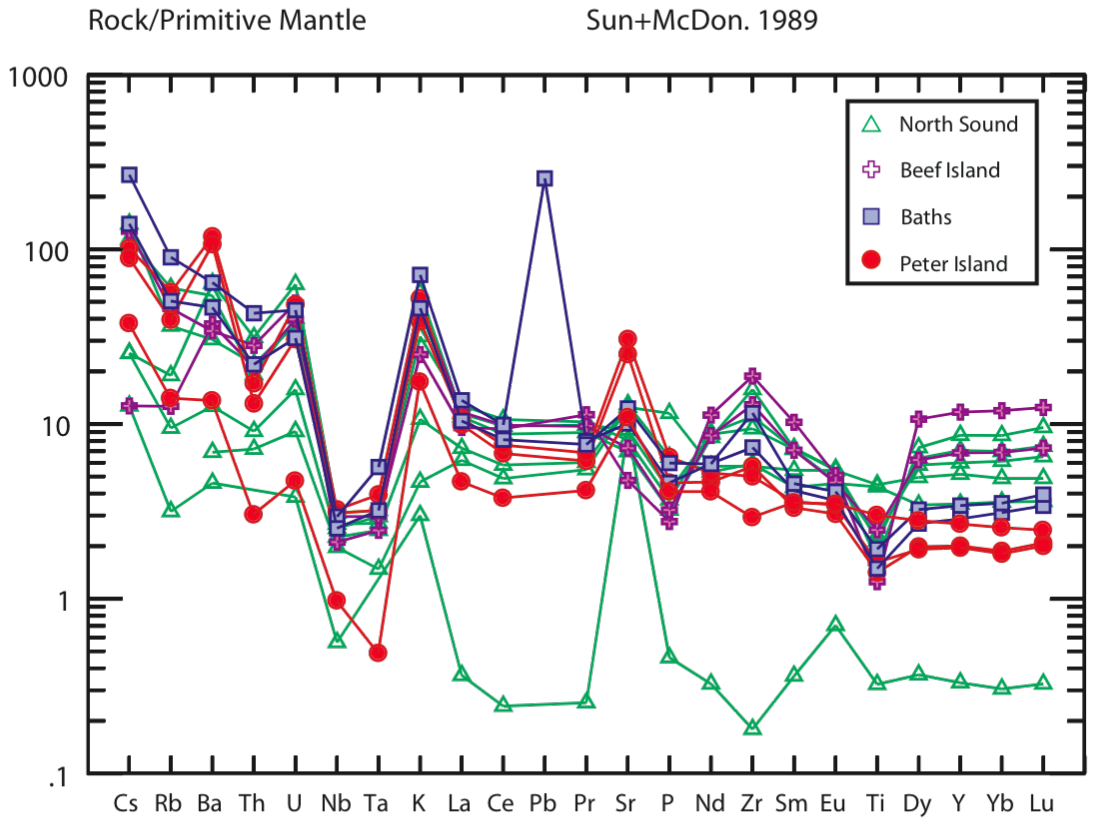

Figure 4: Primitive mantle-normalized trace element patterns for pluton suites of the Virgin Islands batholith. (Primitive mantle-normalizing factors from Sun and McDonough, 1989)

Whole-rock strontium and neodymium isotope geochemistry

$^{87}Sr/^{86}Sr_i$ and $\varepsilon_{Nd}(t)$ are corrected to the crystallization age of the unit from which they belong or to the associated suite age as shown in Table 2 (Fig. 8). $^{87}Sr/^{86}Sr_i$ and $^{143}Nd/^{144}Nd_i$ data overlap with date from the contemporaneous Eocene-Oligocene calc-alkaline rocks of Puerto Rico (Fig. 8). $^{87}Sr/^{86}Sr_i$ data are elevated relative to rocks of the Cretaceous calc-alkaline and Primitive Island Arc series. The North Sound suite has distinctly higher $^{87}Sr/^{86}Sr_i$ values than the younger Peter Island suite.

Whole-rock lead isotope geochemistry

Whole-rock Pb concentrations in all but one sample were below detection limits and isotopic values are presented without age correction. Isotopic growth lines for samples VG-01, BI-26, and PI-13A were calculated; age corrected data will plot along these growth lines depending on the samples U/Pb ratio (Fig. 9). Plutonic rocks of the Virgin Islands batholith span a relatively wide range of present-day Pb isotopic values (Table 3), with $^{206}Pb/^{204}Pb$ (18.76-19.06), $^{207}Pb/^{204}Pb$ (15.61-15.70), and $^{208}Pb/^{204}Pb$ (38.43-38.89). Lead isotope data of the batholith bridge the northern Lesser Antilles and the central and southern Lesser Antilles fields. These data plot above the MORB field towards Atlantic seafloor sediment. The Peter Island suite has the lowest Pb isotopic ratios overlapping with Eocene-Oligocene calc-alkaline rocks of Puerto Rico.

Table 2: Whole-rock Sr and Nd isotopic data

Sample Name	$^{143}Nd/^{144}Nd$	±2s	$^{143}Nd/^{144}Nd_i$	$Nd_{(t)}$	[Nd]	[Sm]	$^{87}Sr/^{86}Sr$	±2s	$^{87}Sr/^{86}Sr_i$	[Sr]	[Rb]	Age (Ma)	Pluton
VG-01	0.512976	0.0007	0.512922	6.64	7.74	2.41	0.704446	0.001052	0.704439	262	<1*	43.6	North Sound
VG-02	0.512976	0.0006	0.512927	6.73	11.30	3.21	0.704295	0.000992	0.704148	146	12	43.6	North Sound
VG-04A	0.512973	0.0008	0.512927	6.73	12.00	3.20	0.704214	0.000968	0.703972	170	23	43.6	North Sound
VG-05	0.512992	0.0006	0.512958	7.19	8.02	1.84	0.704426	0.000951	0.704010	212	57	37.6	Baths
VG-06	0.512983	0.0009	0.512945	6.93	7.97	2.02	0.704165	0.000809	0.703973	258	32	37.6	Baths
VG-09B	0.512903	0.0010	0.512840	5.04	0.44	0.16	0.704087	0.000983	0.704069	194	2	43.6	North Sound
LC-12B	0.512997	0.0008	0.512947	7.09	15.20	4.53	0.704656	0.000756	0.704517	100	8	42.4	Beef Island
PI-13A	0.512179	0.0007	0.512151	-8.74	6.28	1.47	0.704155	0.000784	0.704069	528	36	30.6	Peter Island
PI-13B	0.512978	0.0007	0.512944	6.74	5.60	1.59	0.703943	0.000966	0.703894	232	9	30.6	Peter Island
NI-14A	0.512958	0.0006	0.512931	6.49	7.08	1.59	0.704032	0.000791	0.703983	643	25	30.6	Peter Island
VG-22	0.512993	0.0006	0.512953	7.09	11.80	3.17	0.704420	0.000684	0.704119	195	38	43.6	North Sound
VG-24	0.512953	0.0011	0.512907	6.33	7.18	1.92	0.704032	0.000676	0.703992	272	6	43.6	North Sound
BI-26	0.512961	0.0007	0.512916	6.49	11.60	3.13	0.704508	0.000841	0.704178	153	29	42.4	Beef Island

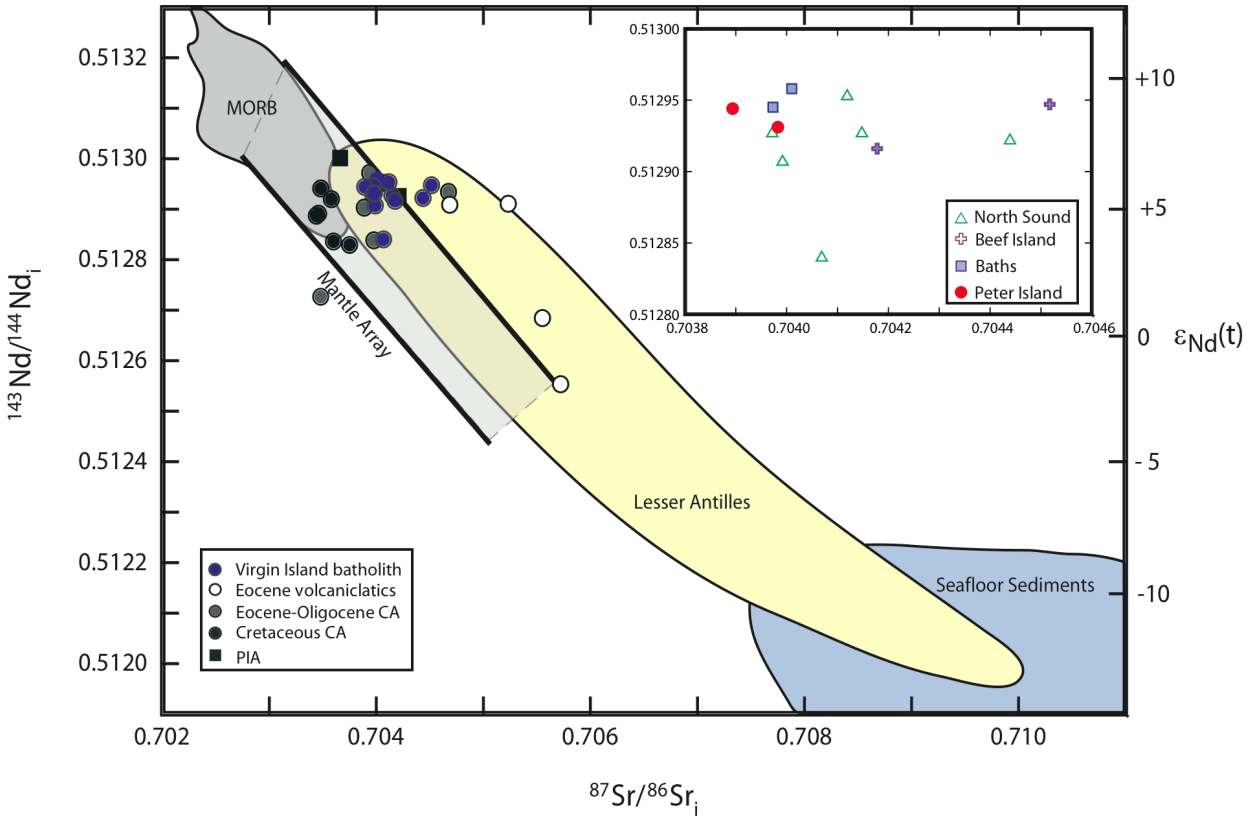

Figure 5: Plot of initial Nd isotope ratios plotted against initial Sr isotope ratios for the data presented in this study. This data is plotted against data fields for Eocene volcaniclastic sediments, Eocene-Oligocene volcanic and pluton rocks of the calc-alkaline association, Cretaceous volcanic and plutonic rocks of the calc-alkaline association, and the volcanic and plutonic rocks of the Primitive island arc association (PIA, Frost et al., 1998). Fields for MORB (White et al., 1987), seafloor sediments of the Barbados Ridge-Demerara Plain (White et al., 1985), and the Lesser Antilles (White et al., 1985) are shown. Inset: $^{143}Nd/^{144}Nd_i$ vs. $^{87}Sr/^{86}Sr_i$ for data presented here. The field for the Mantle Array represents the spectrum of enriched to depleted mantle material. Samples are segregated by each plutonic suite.

Table 3: Whole-rock Pb isotopic data

Sample Name	206 Pb / 204 Pb	±2s	207 Pb / 204 Pb	±2s	208 Pb / 204 Pb	±2s	206 Pb / 207 Pb	±2s	206 Pb / 208 Pb	±2s
VG-01	18.926	0.0053	15.698	0.0069	38.773	0.0086	1.206	0.0022	0.492	0.004
VG-02	19.064	0.005	15.701	0.007	38.893	0.0097	1.214	0.0025	0.494	0.0051
VG-04A	19.052	0.0035	15.670	0.0053	38.810	0.004	1.216	0.0027	0.494	0.0012
VG-05	19.010	0.0077	15.697	0.0099	38.799	0.0121	1.211	0.0025	0.493	0.0048
VG-06	18.946	0.0053	15.650	0.0053	38.637	0.0056	1.211	0.0011	0.494	0.0013
VG-09B	18.850	0.0067	15.657	0.0071	38.633	0.0076	1.204	0.0012	0.491	0.0018
LC-12B	18.918	0.0039	15.653	0.0041	38.678	0.0046	1.209	0.001	0.493	0.0012
PI-13A	18.953	0.0056	15.631	0.0049	38.695	0.0059	1.212	0.0034	0.493	0.0016
PI-13B	18.763	0.0037	15.611	0.004	38.432	0.004	1.202	0.0012	0.492	0.001
NI-14A	18.929	0.0065	15.628	0.007	38.635	0.0069	1.211	0.0013	0.493	0.0016
VG-22	18.943	0.0064	15.662	0.0065	38.700	0.0067	1.209	0.001	0.493	0.0012
VG-24	18.953	0.0071	15.679	0.006	38.781	0.0089	1.209	0.0028	0.492	0.0028
BI-26	19.003	0.0048	15.661	0.0051	38.706	0.0055	1.213	0.0013	0.494	0.0019

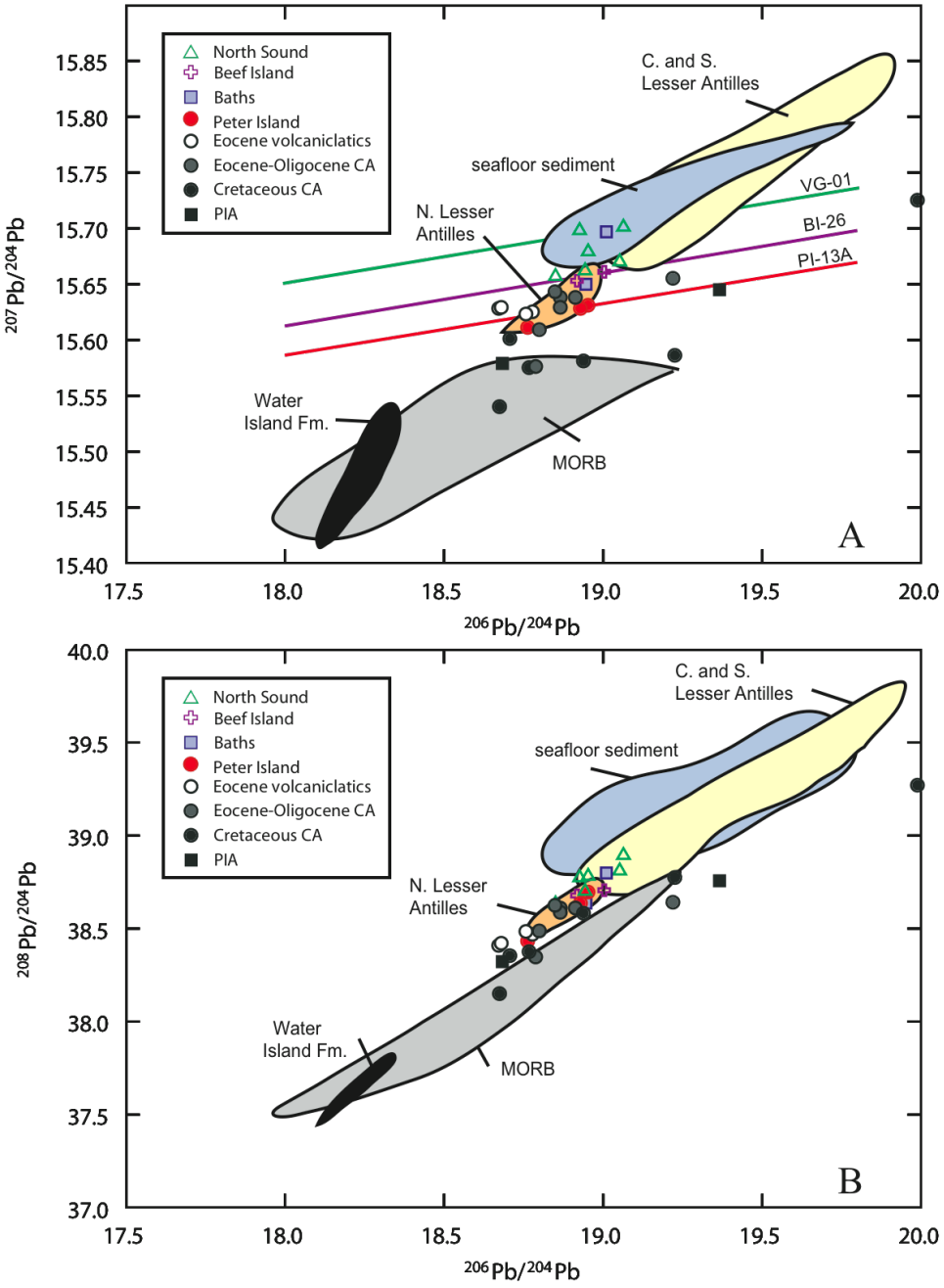

Figure 6: Plot of present-day Pb isotope compositions for data presented in this study. Colored lines in A show the slope of radiogenic growth that has taken place between crystallization and present day for samples VG-01, BI-26, and PI-13A. Initial lead compositions will plot at lower values along these lines based on each sample's U/Pb ratio. Data is plotted against present-day compositions of Eocene-Oligocene volcanic and plutonic rocks of the calc-alkaline association, Cretaceous volcanic and plutonic rocks of the calc-alkaline association, and the volcanic and plutonic rocks of the primitive island arc association (Frost et al., 1998). Also shown are fields for present-day Pb isotopic compositions of MORB (White et al., 1987), seafloor sediments of the Barbados Ridge-Demerara Plain (White et al., 1985), the Lesser Antilles (White and Dupre, 1986; Davidson, 1986, 1987), and the Water Island Formation of the Virgin Islands (Donnelly et al., 1971).

U-Pb zircon geochronology

U-Pb zircon geochronology samples were collected from the North Sound, Beef Island, Baths, and Peter Island suites (Table 4). For each sample, there is a cluster of analyses represented by three or more overlapping data points. The range in $^{206}Pb/^{238}U$ ages and the concordia age of the cluster is reported. Ages from this study suggest an emplacement history spanning at least 13 m.y., from 43.56-30.6 Ma (Fig. 10).

North Sound suite

Four concordant fractions of the quartz diorite phase of the North Sound suite, VG-01, span from 43.53-43.62 Ma. These four fractions, together, yield an age of 43.56 ± 0.08 Ma (MSWD = 0.082).

Beef Island suite

Four concordant fractions of BI-26, the tonalite phase of the Beef Island suite, span from 42.29-42.43 Ma (Fig. 10). LA-ICP-MS of seven zircon grains from BI-26 provides a weighted age of 42.55 ± 0.44 Ma (MSWD = 0.27; C. Allen, personal communication, 2010).

The Baths suite

VG-05 (granodiorite) and VG-06 (tonalite), two geochemically and spatially distinct samples from the Baths suite, yield overlapping ages at approximately 37.6 Ma (Fig. 10). Fractions from these two samples span from 37.37-37.72 Ma. Six concordant fractions of VG-05 cluster and yield an age of 37.62 ± 0.05 Ma (MSWD = 0.53). Two concordant fractions of VG-06 cluster at 37.6.

Peter Island suite

The diorite phase of the Peter Island suite, PI-13A, yields two concordant and two normally discordant fractions of PI-13A spanning 30.62-30.83 Ma, with a $^{206}Pb/^{238}U$ weighted average of 30.6 Ma (Fig. 10). This age is corroborated by LA-ICP-MS of 11 grains from PI-13A giving a weighted mean age of 30.64 ± 0.46 Ma (MSWD = 1.09; C. Allen, personal communication, 2010). One concordant fraction gives an older age of 32.5 Ma, interpreted to reflect inheritance of zircon cores from earlier magmas.

Zircon hafnium and oxygen isotopes

Zircon $\varepsilon_{Hf}(t)$ and $\delta^{18}O$ were analyzed for geochronology samples of the North Sound, Beef Island, Baths, and Peter Island suites (Table 5; Fig. 11). Initial $\varepsilon_{Hf}(t)$ values range from 11.1 to 15.3 and $\delta^{18}O$ values range from 4.3-6.9 per mil. Generally, $\varepsilon_{Hf}(t)$ decreases and $\delta^{18}O$ increases with age. The North Sound, Beef Island, and Baths suites plot within or below the $\delta^{18}O$ field for zircon in equilibrium with mantle-derived melts (Valley et al., 2005). Zircons from the Peter Island suite plot above this field towards crustal values.

TABLE 4. U-PB DATA FOR ROCKS OF THE VIRGIN ISLANDS BATHOLITH

fraction (n)	weight (mg)	conc. (ppm) U	conc. (ppm) Pb*	$^{206}Pb^{\dagger}$ / ^{204}Pb	$^{206}Pb^{\ddagger}$ / ^{238}U	error (%)	$^{207}Pb^{\ddagger}$ / ^{235}U	error (%)	$^{207}Pb^{\ddagger}$ / ^{206}Pb	error (%)	ages (Ma) ^{206}Pb / ^{238}U	ages (Ma) ^{207}Pb / ^{235}U	ages (Ma) ^{207}Pb / ^{206}Pb	corr. coeff.	total common Pb (pg)
VG-01 Quartz diorite of North Sound.															
z1	0.0128	425.4	3.38	1092.0	0.006789	(.21)	0.04384	(.62)	0.00679	(.21)	43.6	43.6	40.5	0.46	2.2
z3	0.0142	375.1	3.00	1598.8	0.006776	(.16)	0.04375	(.38)	0.00678	(.16)	43.5	43.5	40.4	0.52	1.5
z5	0.0117	662.3	5.17	1512.7	0.006776	(.20)	0.04381	(.37)	0.00678	(.20)	43.5	43.5	43.3	0.59	2.2
z6	0.0109	747.3	6.12	1669.8	0.006781	(.23)	0.04389	(0.29)	0.00678	(.23)	43.6	43.6	46.3	0.80	2.1
BI-26 Granodiorite of Beef Island															
z5	0.0326	203.3	1.35	437.4	0.006593	(1.68)	0.04275	(1.69)	0.00659	(1.68)	42.4	42.5	51.1	0.99	6.7
z6	0.0103	518.8	3.39	1342.0	0.006593	(.17)	0.04203	(.33)	0.00659	(.17)	42.4	41.8	10.2	0.56	1.7
z7	0.0280	355.0	2.27	2215.5	0.006604	(.16)	0.04259	(.31)	0.00660	(.16)	42.4	42.4	37.9	0.58	1.9
z12	0.0285	224.0	1.45	831.3	0.006583	(.28)	0.04251	(.54)	0.00658	(.28)	42.3	42.3	40.6	0.56	3.3
VG-05 Granodiorite of the Baths															
z1	0.0390	131.1	0.73	1258.2	0.005836	(.23)	0.03591	(.74)	0.044629425	(.67)	37.5	35.8	75.8	0.44	1.5
z3	0.0424	256.5	2.46	2635.5	0.005815	(.22)	0.03763	(.29)	0.00581	(.22)	37.4	37.5	45.8	0.77	1.5
z6	0.0432	382.6	2.14	1666.8	0.005847	(.23)	0.03782	(.38)	0.00585	(.23)	37.6	37.7	44.6	0.64	3.7
z7	0.0576	403.1	2.29	4504.1	0.005852	(.11)	0.03775	(.15)	0.00585	(.11)	37.6	37.6	38.2	0.74	1.9
z17	0.1178	294.1	1.64	2474.7	0.005868	(.39)	0.03787	(.49)	0.00587	(.39)	37.7	37.7	39.1	0.81	5.3

z20	0.0927	223.8	1.28	1197.5	0.005840	(.61)	0.03771	(.64)	0.00584	(.61)	37.5	37.6	40.7	0.96	6.5
z21	0.0751	303.7	1.73	2594.8	0.005850	(.13)	0.03794	(.17)	0.00585	(.13)	37.6	37.8	50.8	0.77	3.3
VG-06 Granodiorite of the Baths															
z3	0.0371	168.8	1.08	340.8	0.005863	(1.18)	0.03800	(1.25)	0.00586	(1.18)	37.7	37.9	49.7	0.94	7.3
z5	0.0801	103.1	0.59	1467.0	0.005862	(.17)	0.03735	(.56)	0.00586	(.17)	37.7	37.2	8.9	0.41	2.1
PI-13A Diorite of Peter Island															
z1	0.0339	232.8	1.08	2676.8	0.004774	(.17)	0.03065	(.52)	0.00477	(.17)	30.7	30.7	26.9	0.43	0.9
z7	0.0298	387.2	1.79	1223.2	0.004767	(.18)	0.03080	(.25)	0.00477	(.18)	30.7	30.8	42.0	0.75	2.9
z8	0.0292	262.6	1.23	2385.2	0.004761	(.10)	0.03074	(.17)	0.00476	(.10)	30.6	30.7	40.1	0.64	1.0

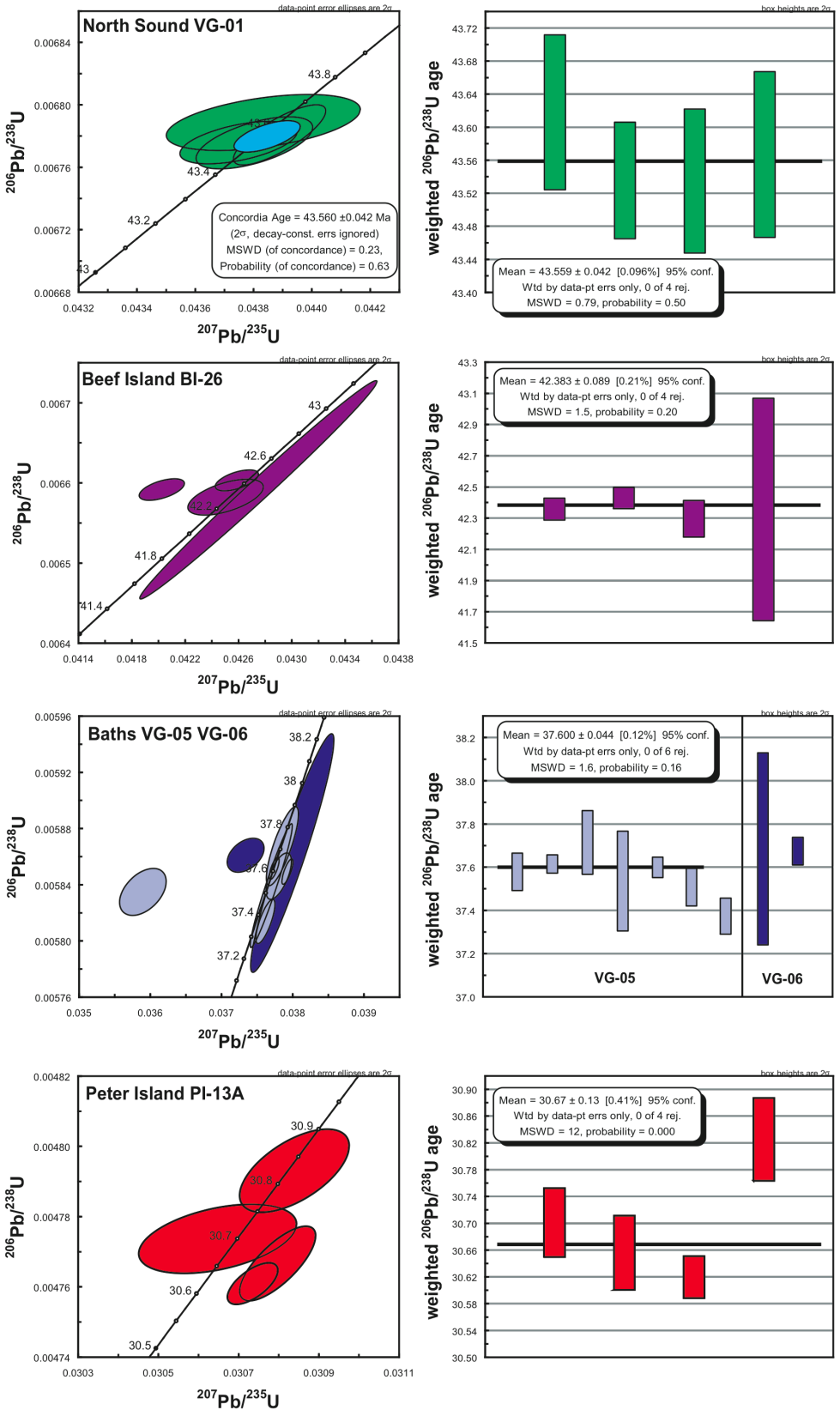

Figure 7: Conventional U/Pb Concordia diagrams for weighted $^{206}Pb/^{238}U$ for zircons analyzed in this study for individual samples of the North Sound, Beef Island, Baths, and Peter Island plutons. Ages reported are weighted mean $^{206}Pb/^{238}U$ ages for a cluster of three or more points and are known to the 2-sigma confidence interval. Data procession and age calculations were completed using the software PbMacDat-2 by D.S. Coleman using the algorithms of Ludwig (1989,1990) and diagrams were constructed using Isoplot v.300 (Ludwig, 2003).

Table 5. ZIRCON HF AND O ISOTOPIC DATA

Sample	$^{176}Hf/^{177}Hf$	$^{176}Hf/^{177}Hf_{(cor)}$	2 S.D.	$^{176}Lu/^{177}Hf$	2 S.D.	U/Pb age(Ma)	1 S.D.	initial epsilon	1 S.D.	$'^{18}O$	1 S.D.
VG-01 Quartz diorite of the North Sound suite											
2	0.283127	0.283148	3.997E-05	0.004108	2.476E-04	43.9	1.1	14.1	1.4	5.3	0.4
8	0.283152	0.283173	3.577E-05	0.003745	1.178E-04	40.2	0.9	15.0	1.3	4.3	0.4
6	0.283144	0.283165	4.026E-05	0.005000	4.472E-05	42.1	0.7	14.7	1.4	5.0	0.4
7	0.283040	0.283060	4.699E-05	0.001718	2.823E-04	41.9	0.8	11.1	1.6	4.3	0.4
BI-26 Granodiorite of the Beef Island suite											
10	0.283127	0.283147	1.882E-05	0.001334	1.365E-05	45.8	0.8	14.2	0.7	5.2	0.4
4	0.283118	0.283139	1.774E-05	0.001709	7.960E-05	43.1	1.5	13.9	0.6	5.4	0.4
5	0.283140	0.283160	2.207E-05	0.001269	5.743E-06	43.4	1.2	14.6	0.8	4.6	0.4
11	0.283148	0.283169	1.435E-05	0.001056	1.348E-05	42.9	0.9	15.0	0.5	4.7	0.4
7	0.283160	0.283181	2.269E-05	0.001613	1.029E-04	41.8	1.1	15.3	0.8	4.7	0.4
3	0.283144	0.283164	1.429E-05	0.001600	1.211E-05	42.6	1.0	14.8	0.5	4.8	0.4
VG-05 Granodiorite of the Baths suite											
3	0.283113	0.283134	1.242E-05	0.000887	1.038E-05	36.6	1.4	13.6	0.4	5.3	0.5
2	0.283136	0.283157	1.567E-05	0.001317	3.341E-05	33.2	1.1	14.3	0.5	4.9	0.4
4	0.283120	0.283141	1.181E-05	0.001212	1.850E-05	34.6	0.8	13.8	0.4	5.2	0.4
VG-06 Granodiorite of the Baths suite											
10	0.283133	0.283154	1.386E-05	0.000947	2.641E-05	40.7	1.4	14.4	0.5	5.2	0.4
8	0.283104	0.283125	1.724E-05	0.000869	2.982E-05	37.4	0.5	13.3	0.6	4.9	0.4
9	0.283096	0.283117	1.660E-05	0.001500	8.703E-05	38.3	1.0	13.0	0.6	5.2	0.4
5	0.283154	0.283175	1.882E-05	0.001735	4.661E-05	36.9	2.0	15.0	0.7	5.3	0.4
2	0.283120	0.283141	1.744E-05	0.000691	4.801E-05	37.5	0.9	13.9	0.6	5.6	0.4
7	0.283154	0.283175	1.768E-05	0.000937	2.303E-05	34.3	0.9	15.0	0.6	5.4	0.4
PI-13A Diorite of the Peter Island suite											
5	0.283116	0.283136	1.428E-05	0.001379	3.326E-05	32.3	0.8	13.6	0.5	6.9	0.4
9	0.283099	0.283120	1.435E-05	0.001285	3.875E-05	29.8	0.6	12.9	0.5	6.1	0.4
10	0.283102	0.283123	1.737E-05	0.001241	2.165E-05	29.8	0.6	13.0	0.6	6.0	0.4
15	0.283130	0.283151	3.163E-05	0.001862	4.751E-05	31.1	0.7	14.0	1.1	5.5	0.4
14	0.283087	0.283107	1.676E-05	0.001166	5.066E-05	31.4	1.3	12.5	0.6	5.8	0.4
13	0.283102	0.283123	1.462E-05	0.001404	2.727E-05	30.6	1.3	13.0	0.5	6.2	0.4

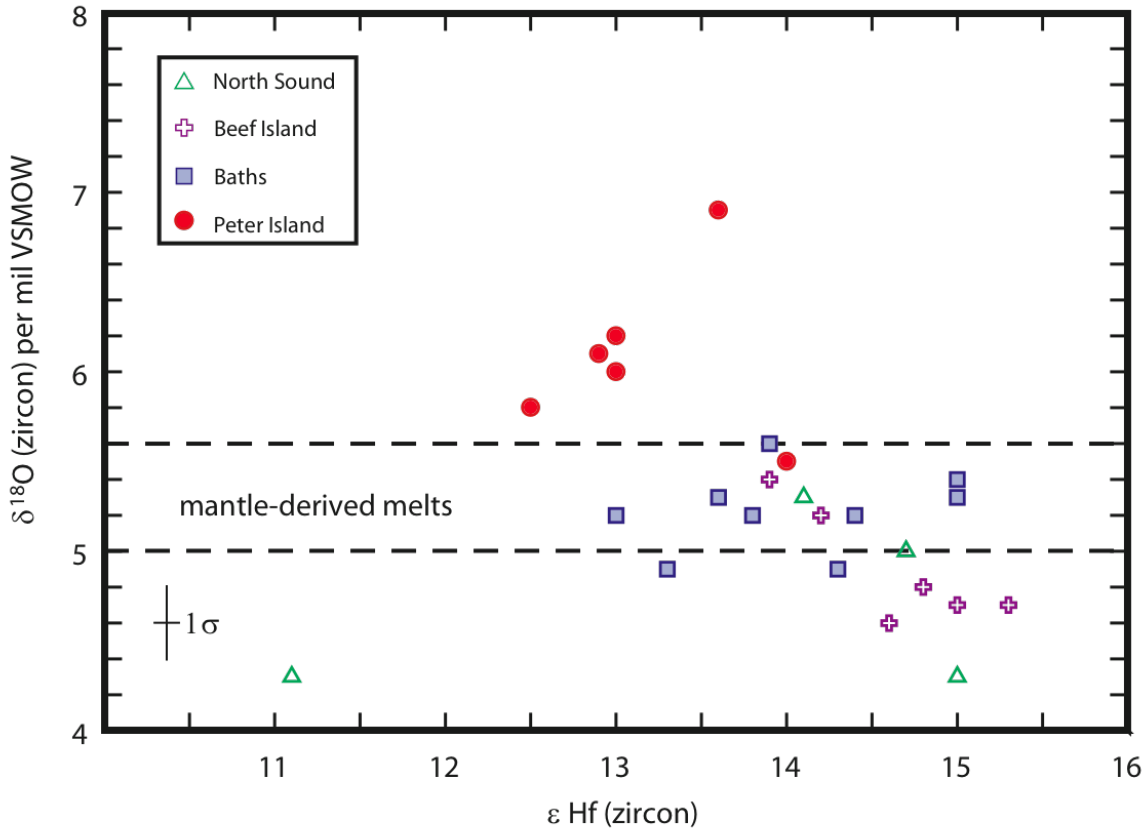

Figure 8: Plot of $\varepsilon_{Hf}(t)$ vs. $\delta^{18}O$ values for zircons of this study. Data from samples of each pluton are assigned the same symbol. Error bars depict 1σ analytical uncertainty. Mantle zircon field represents the range of values for zircons in equilibrium with mantle-derived melts (Valley et al., 2005). VSMOW, Vienna standard mean ocean water.

Chapter 5

Discussion

Trace-element geochemistry

The Virgin Islands batholith comprises a bimodal suite of plutonic rocks. Intermediate compositions, 53 to 62 wt% SiO_2, are either not exposed or were not sampled. Mafic members within the batholith have consistently flat REE patterns (Fig. 6). The character of REE patterns relative to chondrite in the felsic rocks changes with time and falls into two distinct groups. The North Sound and Beef Island suites, 43.6 Ma and 42.4 Ma respectively, display similar patterns. Both suites share negative Eu anomalies and similar enrichments in the light REE (Fig. 6). This REE pattern is suggestive of the removal of plagioclase from these granitic magmas via either fractional crystallization or partial melting of a plagioclase-rich parental body producing mafic cumulates or restites, respectively, in the lower crust (Rudnick, 1992).

Sample VG-09B, a mafic body on western Virgin Gorda at Little Dix Bay, exhibits a depleted REE pattern relative to chondrite that has a pronounced positive Eu anomaly (Fig. 6). This hornblende gabbro, with 42 wt% SiO_2 and high modal plagioclase, displays local modal layering, textural coarsening, and orbicular structures. Geochemical and petrographic features suggest this sample is a gabbroic cumulate (Beard and Day, 1988; Beard and Barker, 1989). A petrogenetic relationship is possible between VG-09B and granitic bodies of the North Sound or Beef Island suites. Mixing between plutons of the North Sound or Beef Island suite with VG-09B produces REE patterns that roughly parallel average arc basalt

(Fig. 12; Peate et al., 1997). The granodiorite plutons of the North Sound suite require VG-09B to comprise ~90% of the bulk composition in order to remove Eu anomalies, whereas the Beef Island suite requires VG-09B to compose 90-95% of the bulk composition. Calculated bulk compositions are depleted relative to average arc basalt but roughly parallel the basalt REE pattern. These calculated bulk compositions are likely too depleted to represent real parental magma compositions and a direct relationship between the gabbroic cumulate, VG-09B, and the granodiorites of either the North Sound or Beef Island suites is unlikely.

REE patterns of the Baths and Peter Island suites, 37.6 and 30.6 Ma respectively, differ from those of the older North Sound and Beef Island suites. These younger suites are enriched in light REE and relatively depleted in heavy REE, creating a concave-up pattern (Fig. 6). The Peter Island suite appears to be slightly less enriched relative to the Baths suite. This concave-up pattern is suggestive of anatectic melting of an amphibolite source (Beard, 1995; Annen et al., 2006; Davidson et al., 2007; Brophy, 2008). The variation in REE patterns correlates to a spatio-temporal distribution within the batholith. Early magmatism demonstrates negative Eu anomalies within a flat REE enrichment pattern and late-stage magmatism exhibits HREE depletion relative to the LREE. This spatio-temporal pattern reflects a transition in the processes producing granitic magmatism in the Virgin Islands batholith through time.

Davidson et al. (2007) demonstrated the use of Dy/Yb and La/Yb versus SiO_2 to differentiate between fractionation trends in arc magmas. Negative correlations of Dy/Yb and positive correlations of La/Yb with SiO_2 indicate the control of amphibole as opposed to flat

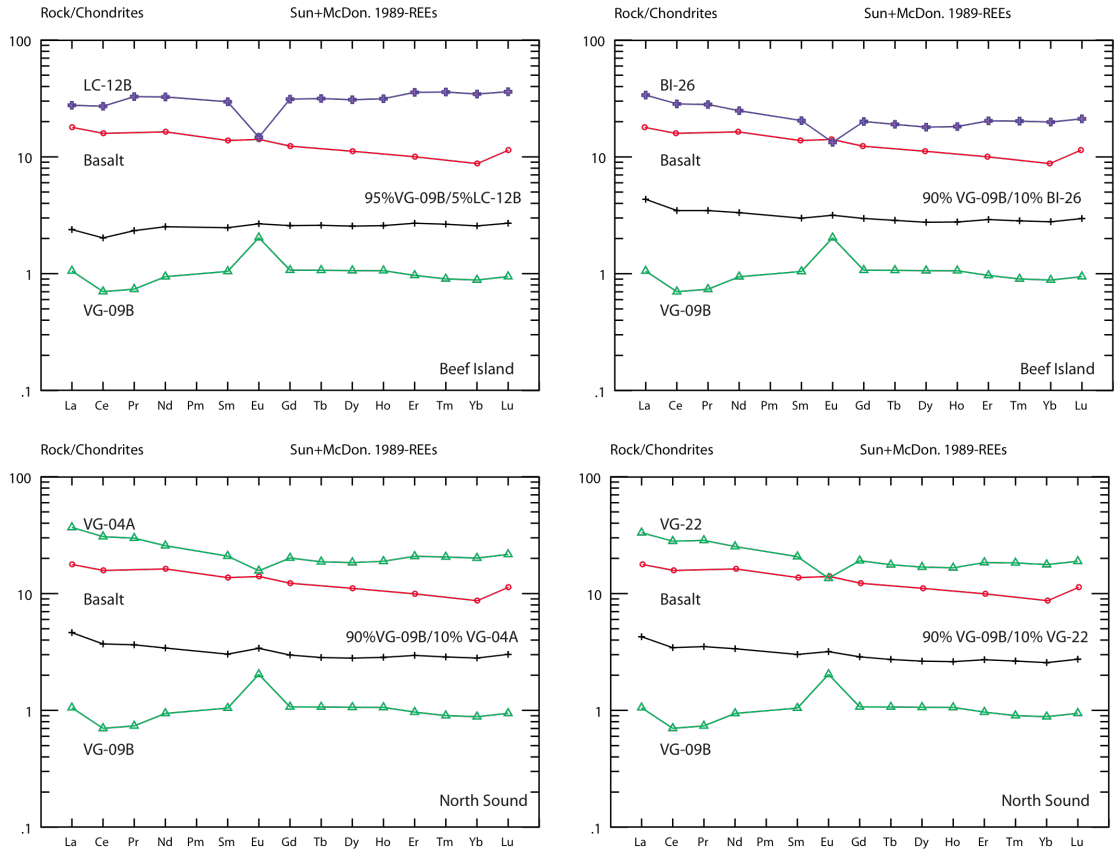

Figure 9: Plot of REE patterns normalized to chondritic values (Sun and McDonough, 1989). Shown are mixing compositions between the cumulate gabbro (VG-09B) and rocks oft he Beef Island suite (LC-12B, upper left; BI-26, upper right) and the North Sound suite (VG-04A, lower left; VG-22, lower right). Also shown is average arc basalt (Peate et al., 1997). Mixing compositions were calculated to determine a parent rock composition assuming the cumulate gabbro was directly related to a granodiorite of the North Sound or Beef Island suite. Compositions were mixed to remove the negative Eu anomalies of the North Sound and Beef Island granodiorites. Calculated compositions approximately parallel average arc basalt composition but are depleted by nearly an order of magnitude.

correlations created by gabbroic (plagioclase-olivine-clinopyroxene) fractionation (Davidson et al., 2007). The Virgin Islands batholith demonstrates a distinct negative correlation between Dy/Yb and SiO_2 (Fig. 13), suggesting that amphibole fractionation has played a significant role in the production of magmas supplying the batholith. However, La/Yb variation within the batholith is not consistent. The North Sound and Beef Island suites exhibit relatively flat differentiation trends consistent with gabbroic fractionation, whereas the Baths and Peter Island suites display increasing La/Yb with SiO_2 consistent with amphibole fractionation trends (Fig. 13; Davidson et al., 2007). These results show a temporal variation in differentiation trends within the Virgin Islands batholith with early magmatism dominated by plagioclase fractionation producing the negative Eu anomalies in the felsic intrusive of the North Sound and Beef Island suites. The late stage magmatism of the Baths and Peter Island suites appear to lack the influence of plagioclase fractionation. This difference in differentiation trends between early and late stage magmatism may reflect changing conditions during the time of emplacement as the arc crust continued to thicken.

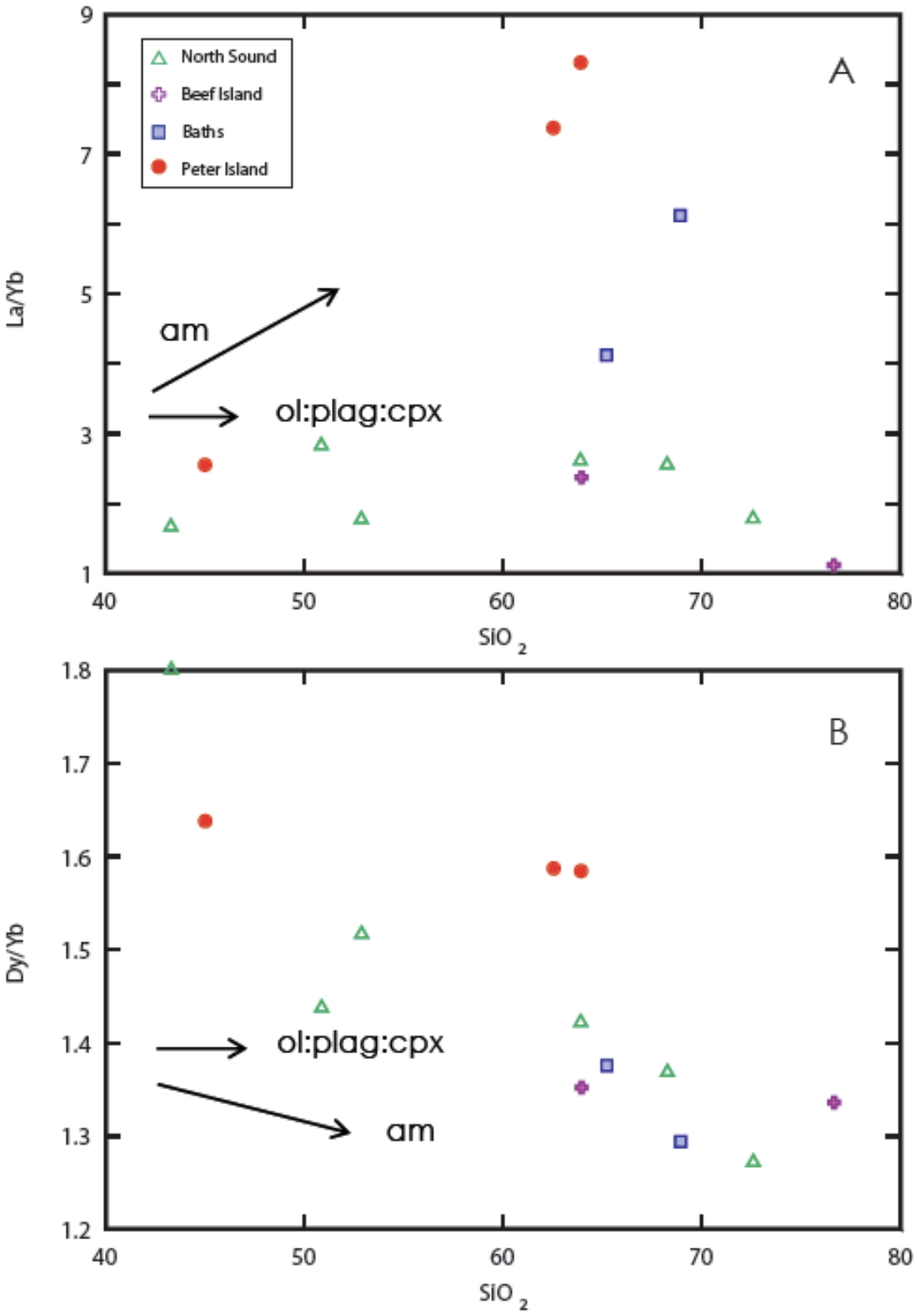

Figure 10: Plot of $Si0_2$ concentration (wt. %) vs. La/Yb ratio (A) and Dy/Yb ratio (B). Data shown are segregated for each plutonic suite. Also shown are the approximate fractionation trends for amphibole (am) and gabbro (ol:plag:cpx) after Davidson et al., (2007).

Isotope geochemistry

Strontium and Nd isotopic values within the Virgin Islands batholith are relatively less evolved in comparison to other arc magmas depicted in Figure 8. These primitive values suggest a largely mantle-derived origin with little incorporation of isotopically evolved crustal material or influence from sediment or slab derived fluids. However, recycling of early magmatic products is likely as evidenced by inherited zircon ages from the North Sound and Peter Island suites.

Frost et al. (1998) characterized the Cretaceous and Paleogene volcanic and plutonic rocks from Puerto Rico using Nd, Sr, and Pb isotopic data and grouped them in relation to the primitive island arc and calc-alkaline associations. These associations were used to separate three subgroups: the primitive island arc samples; the Cretaceous calc-alkaline samples; and the Eocene-Oligocene calc-alkaline samples. The primitive island arc association is distinguished by radiogenic initial Nd ratios, Pb isotopic ratios ranging from MORB-like unradiogenic to more radiogenic Pb isotope ratios. The Cretaceous calc-alkaline rocks have slightly less primitive initial Nd isotope ratios. The Eocene-Oligocene rocks have roughly similar initial Nd isotope compositions and more radiogenic initial Sr isotope compositions than the Cretaceous primitive island arc and calc-alkaline associations.

Similar to the Eocene-Oligocene calc-alkaline association in Puerto Rico, the Virgin Islands batholith has elevated $^{87}Sr/^{86}Sr_i$ relative to the Cretaceous calc-alkaline and primitive island arc association. This variation is likely due to incorporation of slab or sediment-derived fluids carrying fluid mobile large ion lithophile elements including isotopically enriched Sr. Within the batholith, there is little isotopic variation; however, the older North Sound and Beef Island exhibit elevated $^{87}Sr/^{86}Sr_i$ values relative to the younger Baths and

Peter Island suites. Why this enrichment would decrease with time is unclear; however, this internal variation may be the result of decreased incorporation of subduction-derived fluids in the genesis of the batholith over time as subduction transitioned from perpendicular to oblique and on to sinistral transtension.

Modern whole-rock Pb isotope values of Cretaceous, Eocene, and Oligocene calc-alkaline rocks of Puerto Rico and the Virgin Islands overlap with Plutonic rocks of the Virgin Islands batholith; however, values from the batholith extend to more isotopically enriched Pb isotope values overlapping with data from the northern Lesser Antilles volcanic rocks (Fig. 9). The Cretaceous Water Island Formation is significantly less isotopically enriched than the Virgin Islands batholith, overlapping the field of MORB values. The central and southern Lesser Antilles extends to Pb isotope compositions that are greatly enriched relative to those of the Virgin Islands batholith. The Pb isotopic character of Lesser Antilles lavas show a decrease in Pb isotopic values from south to north that has been interpreted to reflect a decrease in the amount of subducted terrestrial-derived sediments and arc crust incorporated into the arc magmas (Davidson, 1987; White and Dupré, 1986). Frost et al. (1998) concluded the amount of terrigenous material incorporated into Puerto Rican arc magmas was similar to or slightly greater than the amount incorporated into arc magmas of the northern Lesser Antilles. This conclusion is consistent with Pb isotopic values from the Virgin Islands batholith; however, within the Virgin Islands batholith lead isotopic values of the suites appear to become less enriched with age, most notably between the North Sound and Peter Island suites. This trend mimics that seen in the $^{87}Sr/^{86}Sr_i$ values and supports the hypothesis that the incorporation of crustal material or subduction-derived fluids decreased with time in the Virgin Islands batholith.

Zircon $\varepsilon_{Hf}(t)$ and $\delta^{18}O$ data support derivation of the Virgin Islands batholith from a mantle-derived source (Fig. 11). A narrow range of $\delta^{18}O$ (5.3±0.3 per mil) values characterizes zircon in equilibrium with mantle-derived melts; values greater than 5.6 per mil indicate incorporation of isotopically enriched crustal components (Valley et al., 2005; Kemp et al., 2007). The Virgin Islands batholith exhibits increasing $\delta^{18}O$ with decreasing $\varepsilon_{Hf}(t)$ and age (Fig. 11). Older suites express $\delta^{18}O$ values of zircon in equilibrium with those that are characteristic of mantle-derived melts whereas younger suites exhibit increasingly more positive $\delta^{18}O$ values and lower $\varepsilon_{Hf}(t)$, evidence of increasing incorporation of crustal components. Zircons with values plotting below the field of values in equilibrium with mantle-derived melts trend toward VSMOW and may be contaminated by meteoric sources (Bindeman, 2008). Within the batholith $\varepsilon_{Hf}(t)$ and $\varepsilon_{Nd}(t)$ appear not to agree (Fig. 14). Continental crust should evolve towards more negative $\varepsilon_{Nd}(t)$ and $\varepsilon_{Hf}(t)$ values; however, the younger continental-like Baths suite has more positive $\varepsilon_{Nd}(t)$ and slightly less positive $\varepsilon_{Hf}(t)$values creating a slope that is opposite that of what should be expected of maturing arc crust. This could be the result of a decoupling of the Hf and Nd isotopic systems if garnet was present during melting. Melting with garnet present would preferentially retain Lu and Hf relative to Sm and Nd and potentially changing the dynamics of $\varepsilon_{Nd}(t)$ whole rock and $\varepsilon_{Hf}(t)$ zircon correlations (Rubatto and Hermann, 2007)).

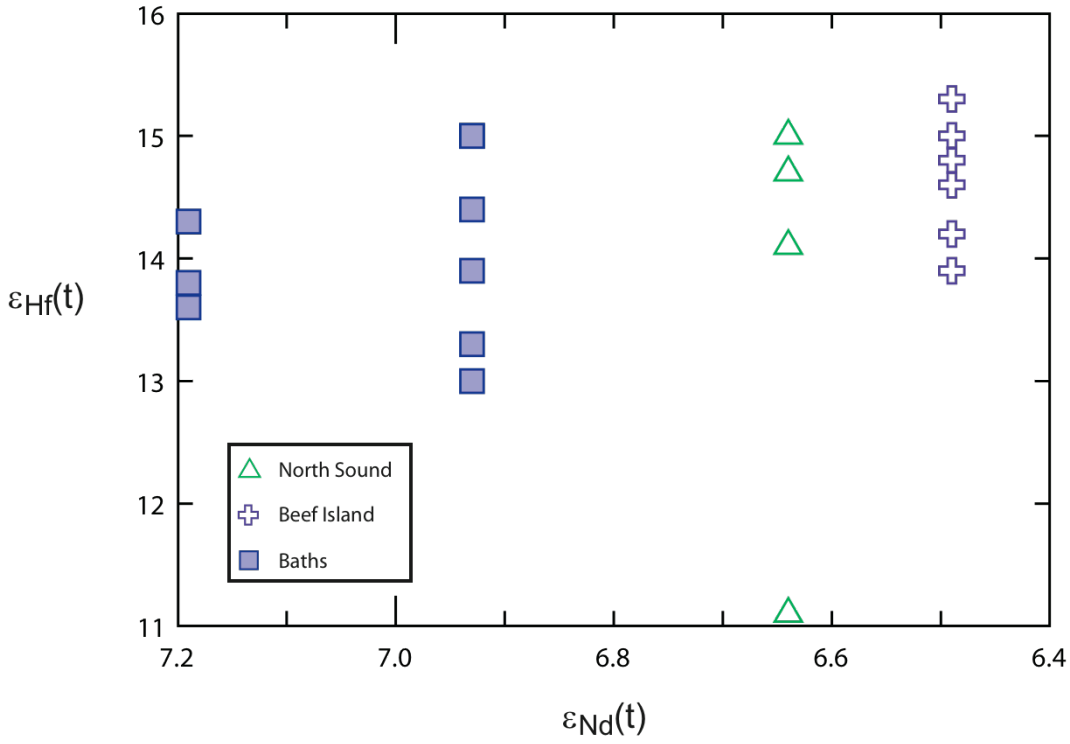

Figure 11: Plot of whole rock $\varepsilon_{Nd}(t)$ vs. zircon $\varepsilon_{Hf}(t)$ for selected samples the North Sound (VG-01), Beef Island (BI-26), and the Baths (VG-05, VG-06) suites. The Peter Island suite is excluded due the lack of whole rock $\varepsilon_{Nd}(t)$ values.

Emplacement of the batholith

Early studies suggested that the Virgin Islands batholith was emplaced in a single Eocene event (Longshore, 1965; Helsley, 1971). However, U-Pb geochronology from this study demonstrates that the batholith was emplaced over a period of ≥13 m.y. (Fig. 10). The batholith becomes younger to the south-southwest with an apparent lateral magmatic migration rate of approximately 1.8mm/yr. Kesler and Sutter (1979) reported a hornblende Ar-Ar total gas age of 24.3 Ma for a quartz diorite in the Narrows, between Tortola and St. John (Fig. 3). If this age represents a crystallization age, it extends the duration of emplacement to approximately 19 m.y. and continues the trend of younging magmatism to the south-southwest.

Helsley (1960) originally described the emplacement of the batholith as a series of large sill-like sheets intruded parallel to the bedding of metasedimentary rocks. Helsley (1960) and Longshore (1965) made this interpretation based on stratification of gabbros and diorites that now appear to be vertical or overturned with an attitude similar to bedding of metasedimentary rocks. After the batholith was emplaced, regional deformation created a northward dipping homocline with the dip of metasedimentary rocks systematically varying south to north from 50°S (overturned) to 15°N (Helsley, 1971). Helsley (1971) supported this interpretation with rock magnetism measurements on dikes and batholithic rocks showing a minimum rotation of metasedimentary rocks 80 to 90° about an axis approximately parallel to strike (N70°W to N60°E).

The Peter Island suite is a series of mafic, tonalite, and diorite sheets with internal chilled margins suggesting its emplacement in a shallow sub-volcanic system. This observation implies the Peter Island suite was not emplaced by the same mechanism as the

rest of the batholith or the batholith itself was not emplaced as a downward stacking sill complex.

The spatio-temporal pattern of emplacement within the Virgin Islands may be explained by an alternative model. Subduction erosion of the fore-arc provides an effective mechanism in which to transport intrusive bodies trenchward (von Huene and Scholl, 1991). During the formation of the batholith, a trench was located to the north-northeast of the present day Virgin Islands (Jolly et al., 1998b). Trenchward migration would create a south-southwest migration of magmatism within the Virgin Islands batholith. The lateral migration of magmatism within the batholith is consistent with subduction erosion at a trench to the northeast of the present day Virgin Islands. Crustal recycling caused by subduction erosion at the forearc may provide a mechanism by which crustal materials were incorporated into the magmas that created the Virgin Islands batholith. The transition from perpendicular and oblique subduction to sinistral transtension along the Puerto Rico trench likely resulted in decreased recycling of the forearc during the production of the Virgin Islands batholith. This decrease in isotopically enriched material incorporated into subduction-derived fluids may correlate to the observed decrease in the isotopic enrichment of Sr and Pb between the older North Sound and Peter Island suites.

Continental crust formation

The processes controlling the distillation of the continental crust from the mantle remain heavily debated. Early hypotheses for the creation of felsic continental crust suggest a single-stage process dominated by magmatic differentiation from mafic magmas (Bowen, 1928). Recent models suggest a multi-stage process involving hydration and partial melting of mafic crustal rocks, intracrustal differentiation, hybridization, crustal reworking, chemical

weathering of surface rock, subduction of these sediments and altered oceanic crust, and delamination of dense mafic lower crustal residues (Rudnick, 1995; Albarède, 1998; Annen et al., 2006; Lee et al., 2006).

Models of continental crust formation are based on observations of upper crustal rocks and lower crustal models based on exposed granulite terranes, seismic velocities, and heat flow observations (e.g. Weaver and Tarney, 1984; Rudnick and Fountain, 1995; Taylor and McLennan, 1995; Wedepohl, 1995). These models estimate andesitic bulk compositions created by the accretion of oceanic island arcs; however, these arcs are dominated by mafic end-members.

The trondhjemite-tonalite-granodiorite (TTG) series that dominates Achaean cratons marks the transition from early mafic crustal components to more felsic continental crust (Rapp et al., 1991; Rudnick, 1995; Smithies et al., 2003). Tonalites and granodiorites of the Virgin Islands batholith are similar to the average Achaean TTG with respect to major- and trace-element variations and are less enriched in incompatible trace elements relative to modern upper continental crustal average. However, Achaean TTG compositions are enriched in incompatible trace-elements and light REE but depleted in heavy REE relative to the Virgin Islands batholith (Fig. 15-16).

On average, the granitic rocks of the Virgin Islands batholith have continental-like trace-element signatures (Fig. 16). Variations from average continental crust and upper continental crust show that the batholith is depleted in Cs, Nb, and Ta as well as the light REE. Depletion of Nb and Ta are typical of subduction-derived magmatism and depletion of Nb relative to the light REE is indicative of crustal growth at convergent margins as opposed to intraplate settings (Barth et al., 2000). Whereas the granitic rocks of the Virgin Islands

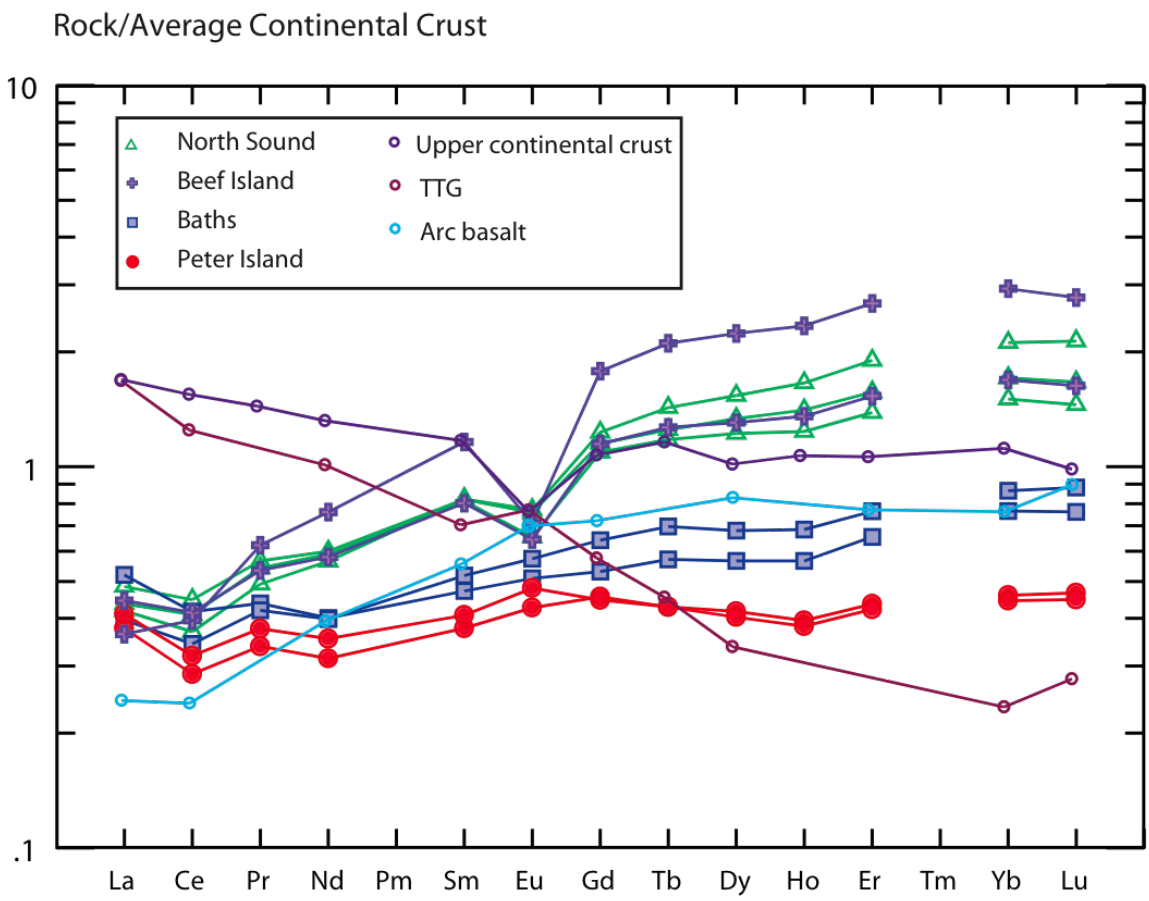

Figure 15: Plot of rare earth element patterns for granodiorites of the Virgin Islands batholith normalized to average continental crust (Rudnick and Fountain, 1995). Also shown are the average upper continental crust (Taylor and McLennan, 1985), average Achaean TTG (Drummond et al., 1996), and average arc basalt (Peate et al., 1997).

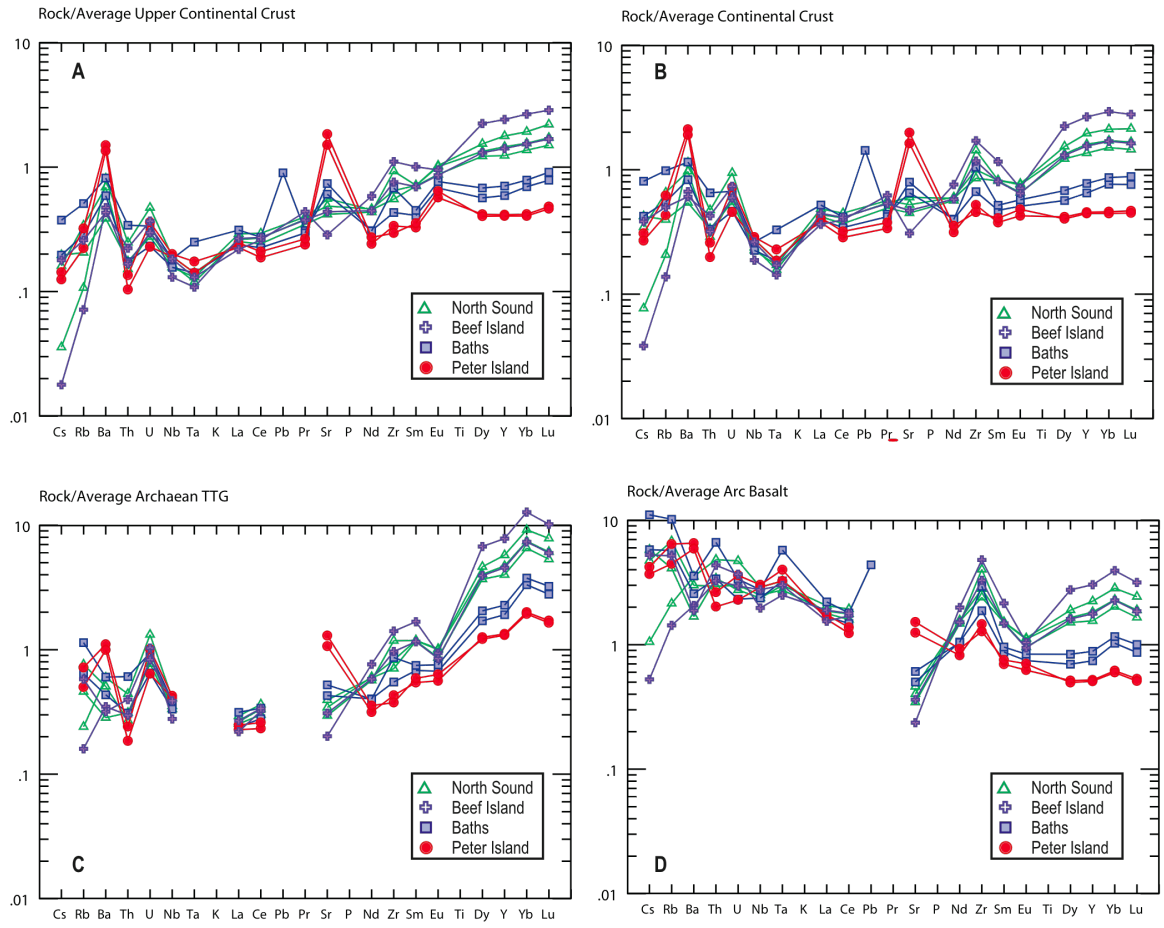

Figure 16: Plot of trace-element patterns of the granitic rocks of the Virgin Islands batholith normalized to A) average continental crust (Rudnick, 1995), B) upper continental crust (Taylor and McLennan, 1985), C) average TTG (Drummond et al., 1996), and D) average arc basalt (Peate et al., 1997). Trace-element order after Sun and McDonough (1989).

batholith are depleted in Cs, Nb, and Ta, and ratios of La/Nb and Nb/Ta resemble bulk and upper continental crust values while maintaining more primitive Nb concentrations (Fig. 17; Barth et al., 2000).

The Virgin Islands batholith becomes more like continental crust over time with respect to REE and trace element patterns. Early granodiorites resemble average arc basalts and largely parallel trace element patterns whereas late-stage granodiorites resemble continental crust. REE patterns of the younger Baths and Peter Island suites roughly parallel average continental crust (Fig. 15). This temporal trend can be seen using the Rb/Lu ratio across the suites of the batholith, which become progressively more like continental crust with age (Fig. 18). Early granodiorites of the Virgin Islands batholith resemble basalts whereas late-stage granodiorites evolve towards average upper continental crust values.

Exposure of middle and lower crustal plutonic rocks in oceanic island arcs also occur in Talkeetna, Alaska (e.g. Beard and Barker, 1989; DeBari and Sleep, 1991; Greene et al., 2006); Kohistan, Pakistan (e.g. Khan et al., 1993; Jagoutz et al., 2006; Jagoutz et al., 2009); and Fiji (Gill and Stork, 1979; Stork, 1984). Compositions within the Virgin Islands batholith overlap consistently with these plutonic rocks, with minor variations in the incompatible elements (Fig. 19). Evidence from the Virgin Islands batholith and global oceanic arc terranes of the Greater Antilles, Talkeetna, Kohistan, Fiji, and the Scotia arc demonstrate the ability of mature oceanic island arcs to produce continental-like granites. These terranes are composed of granites with similar major- and trace-element compositions (Fig. 19) and are generally less enriched in incompatible elements than average upper crustal compositions.

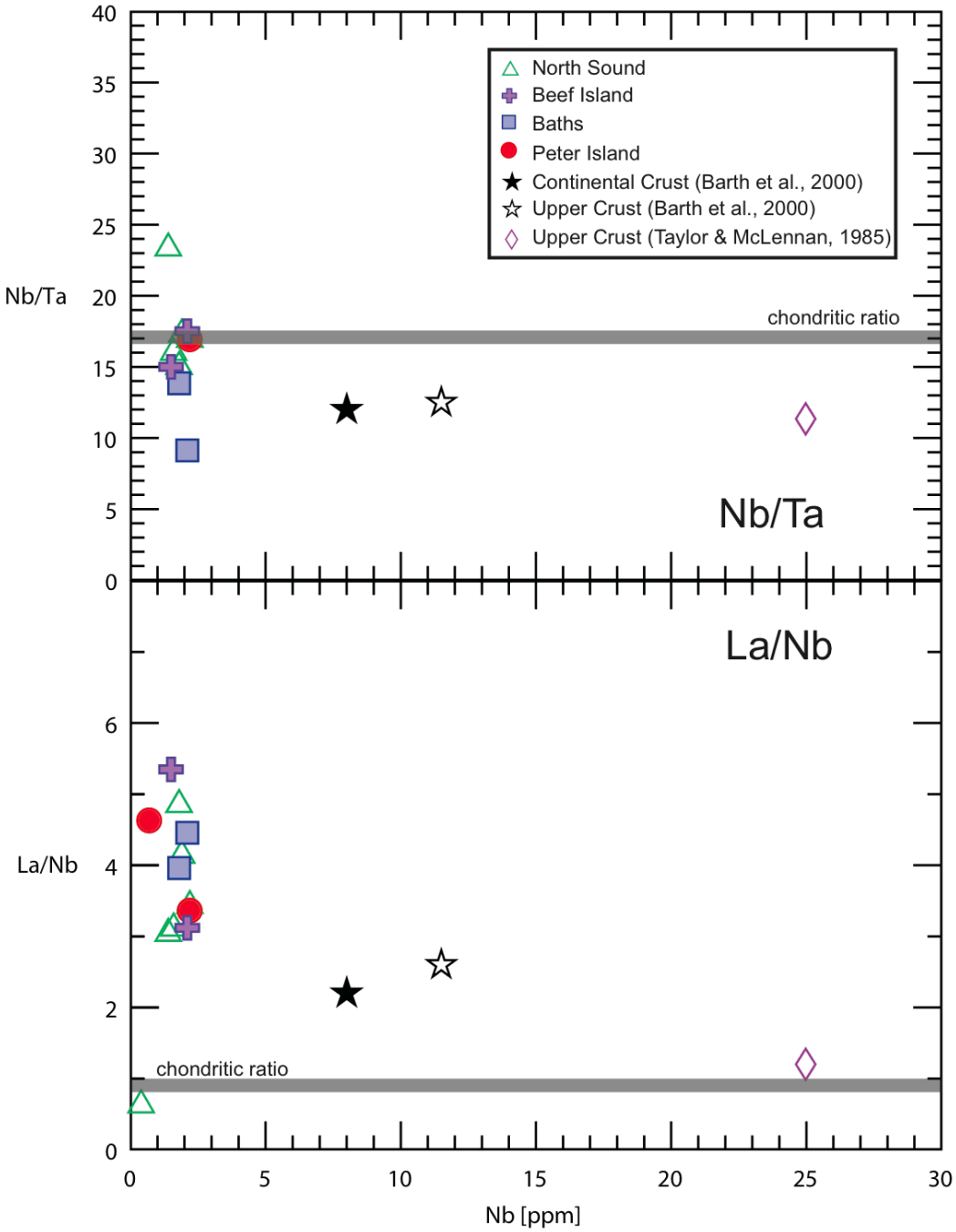

Figure 17: Plot of Nb concentration vs. Nb/Ta ratio (upper panel) and La/Nb ratio (lower panel) for the plutonic rocks of the Virgin Islands batholith after Barth et al., 2000. Also shown are the chondritic ratios (gray bars; Jochum et al., 1997; McDonough and Sun, 1995), the upper continental crust (black empty star) and average continental crust (black filled star) values of Barth et al. (2000); and the upper continental crust (purple diamond) of Taylor and McLennan (1985).

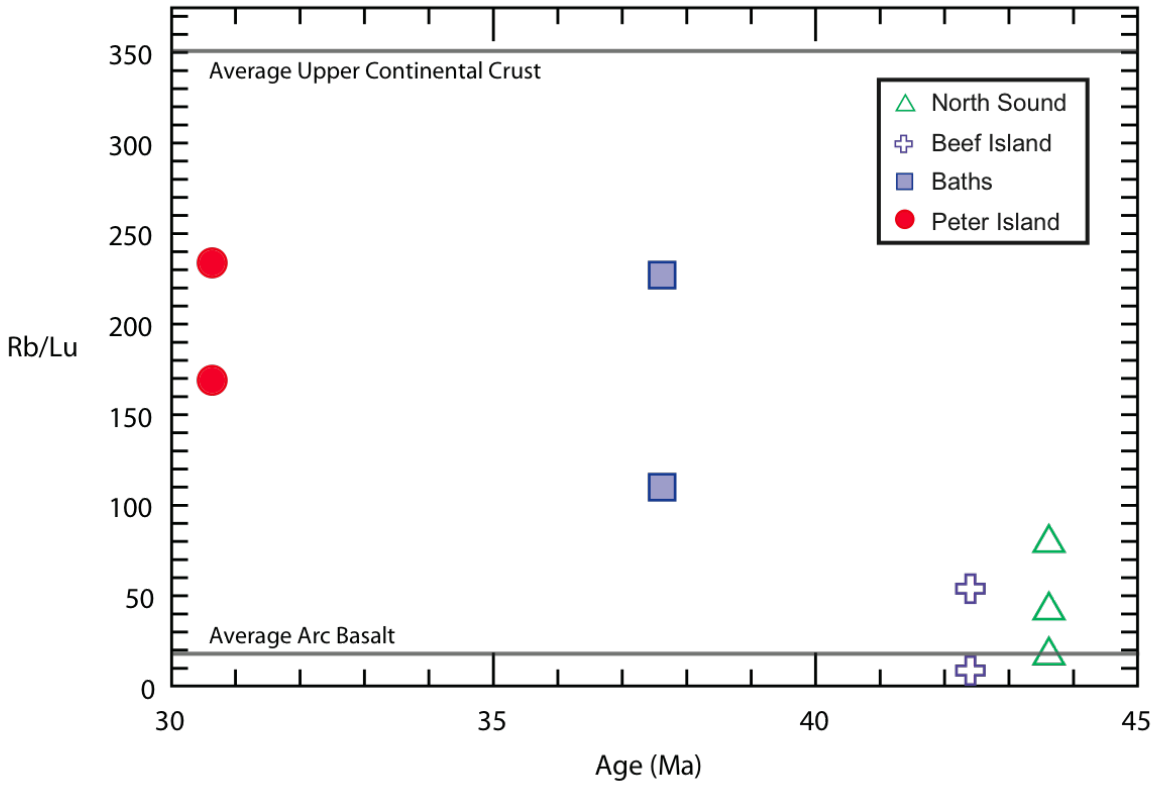

Figure 12: Plot of age (Ma) vs. Rb/Lu ratio)for the granodiorite bodies of the Virgin Islands batholith. Granodiorites of the Virgin Islands batholith become progressively more crustal with time. Data is compared to Rb/Lu values for average upper continental crust (Taylor and McLennan, 1985) and average arc basalt (Peate et al., 1997).

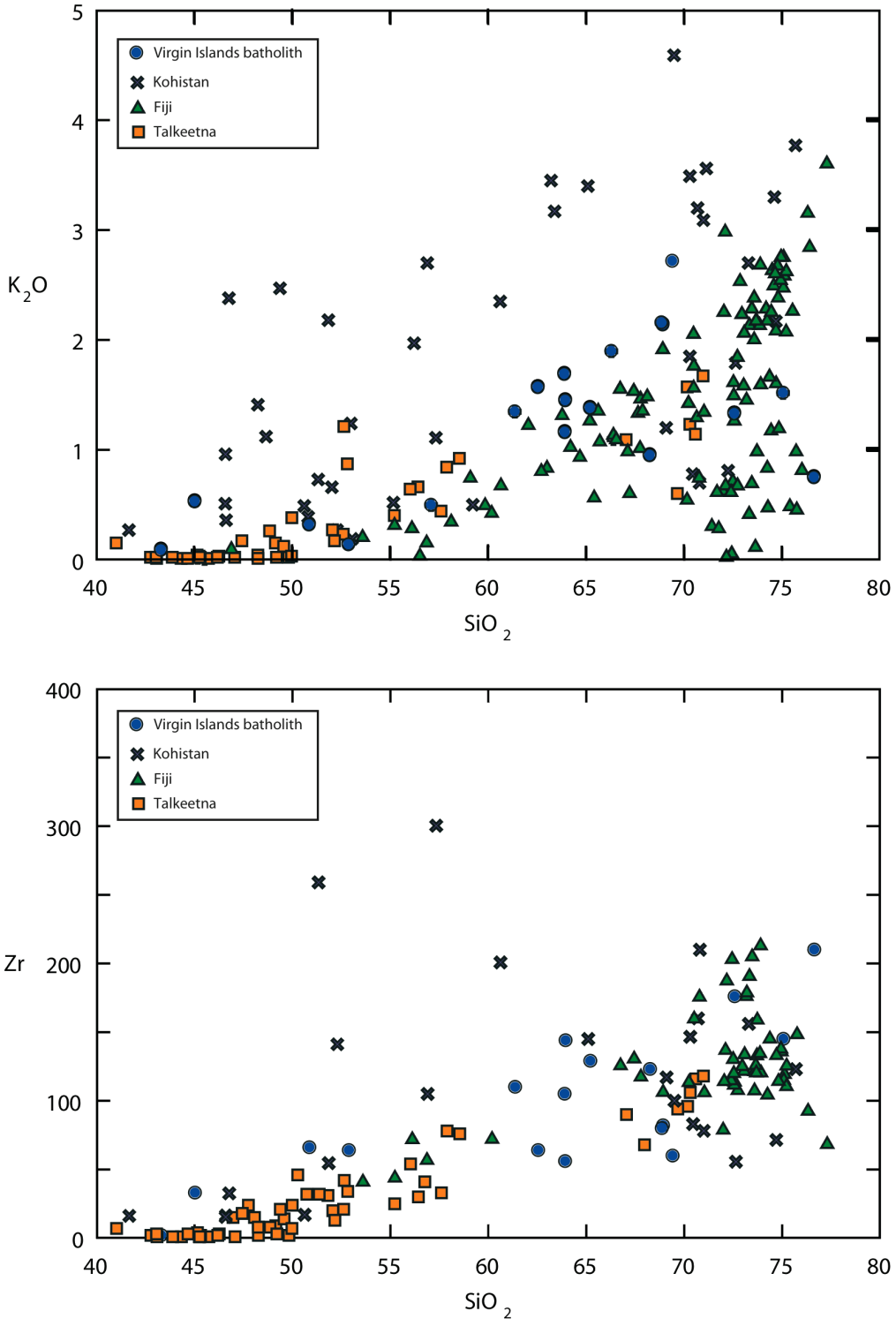

Figure 19: Plot of SiO_2 concentration vs. K_2O (upper panel) and Zr (lower panel) concentrations of the Virgin Islands batholith compared to felsic plutonic rocks from Kohistan (Khan et al., 1993; Jagoutz et al., 2006, 2009), Talkeetna (Beard and Barker, 1989; DeBari and Sleep, 1991; Greene et al., 2006), and Fiji (Gill and Stork, 1979; Stork, 1984). K_2O and SiO_2 in weight percent, Zr in parts per million.

Crustal additions similar to the granodiorites of the Virgin Islands batholith move the average composition of island arc terranes towards average continental values. However, the Virgin Islands batholith does not have the level of LREE enrichment needed to account for concentrations in average continental crust. LREE enrichment in Fiji, Talkeetna, and Kohistan approach or exceed the level of enrichment found in average continental crust. In order to derive the trace element concentrations of average continental crust from the granodiorites of the Virgin Islands batholith requires melting of approximately 50 percent. Smaller degrees of melting will produce trace element concentrations that are enriched relative to average continental crust.

Evidence from these arc terranes suggest long-lived oceanic island arcs evolve towards continental-like compositions producing isotopically primitive granitic plutons at mid-crustal depths and contributing to crustal thickness and maturation of oceanic island arcs (Hamilton, 1981; Jagoutz, et al., 2009). This continental-like crust is likely a precursor or nascent form of continental crust that has yet to undergo further differentiation during continued arc magmatism and reworking during arc accretion.

Chapter 6

Conclusions

The Virgin Islands batholith was emplaced over a period of at least 13 m.y., from 43.6 to 30.6 Ma. Emplacement occurred either as a series of downward stacking sills or as a series of dike-like intrusion that migrated trenchward during subduction erosion, creating the current pattern of lateral south-southwest migration. Structural and paleomagnetic evaluations of the batholith are needed for a more precise correlation of spatial and temporal data, leading to a more comprehensive model of emplacement.

The spatio-temporal pattern within the batholith is accompanied by a transition in REE patterns with early magmatism characterized by negative Eu anomalies and younger magmatism by heavy REE depletion. Dy/Yb correlations with silica indicate that magmatism fueling the Virgin Islands batholith originated from anatectic melting of stockpiled basalts or amphibolites at lower and mid-crustal depths. Plagioclase fractionation in the early magmatism that created the North Sound and Beef Island suites produced negative Eu anomalies.

Strontium and Nd whole-rock isotopic data along with zircon Hf and O isotopic data demonstrate the primitive nature of the Virgin Islands batholith. These primitive values indicate mantle-derived sources with minimal incorporation of crustal components with enriched isotopic character. Zircon Hf-O isotopic data suggest increased incorporation of crustal components throughout evolution of the batholith.

Granitic rocks of the Virgin Islands batholith become progressively more like continental crust through time. This is demonstrated by the spatio-temporal evolution of REE and trace-element patterns that evolve from basalt-like toward average continental crust. These nascent crustal rocks represent a unique stage in the development of continental crust and carry similarities to both end of the crustal spectrum.

The Virgin Islands batholith is similar in composition to global accreted oceanic island arc terranes. Granitic plutons with primitive isotopic compositions are emplaced at mid-crustal depths within these arcs and approach the levels of incompatible enrichment found in average continental crust. Oceanic island arcs mature toward typical continental crust and represent the nascent stages of continent building requiring isotopic enrichment and further incompatible element enrichment during accretion and continued continental arc magmatism.

Appendix:

Locations and descriptions of samples collected. Rock names after IUGS QAP classification.

VG-01 LAT (N) 18°29'12.24" LONG (W) 64°23'18.87"

Virgin Gorda. Along road cut by the Police Station in North Sound.

Quartz diorite. Plagioclase (78.6%), quartz (8.3%), and amphibole (3.8%) with secondary sericite and chlorite (9.3%).

VG-02 LAT (N) 18° 29' 48.92" LONG (W) 64° 23' 9.49"

Virgin Gorda. Behind grocery store in Leverick Bay.

Fine-grained tonalite. Plagioclase (47.9 %), quarts (34%), potassium feldspar (8.1%), amphibole (18%), and opaque mineral (2.7%). Iron staining, sericite, chlorite (3.9%), and altered biotite.

VG-03A LAT (N) 18° 29' 31.22" LONG (W) 64° 24' 1.26"

Virgin Gorda. Along dirt road cut west of South Sound. Heavily faulted heterogeneous unit with veins of amphibole, epidote, and felsic dikes.

Tonalite. Plagioclase, quartz, potassium feldspar and opaque minerals. Secondary chlorite alteration and iron oxidation.

VG-03B LAT (N) 18° 29' 31.22" LONG (W) 64° 24' 1.26"

Virgin Gorda. Along dirt road cut west of South Sound. Heavily faulted heterogeneous unit with veins of amphibole, epidote, and felsic dikes.

Amphibole veins in VG-03A. Amphibole, plagioclase, opaques, and quartz. Chlorite alteration.

VG-03C LAT (N) 18° 29' 31.22" LONG (W) 64° 24' 1.26"

Virgin Gorda. Along dirt road cut west of South Sound. Heavily faulted heterogeneous unit with veins of amphibole, epidote, and felsic dikes.

Mafic dike. Amphibole, plagioclase, biotite, opaque minerals, Secondary chlorite alteration.

VG-04A LAT (N) 18° 29' 53.48" LONG (W) 64° 24' 26.71"

Virgin Gorda. Along dirt road on the western coast of Virgin Gorda north of Plum Tree Bay.

Tonalite with enclaves (variable). Color index increases to the south. Plagioclase (58.8%), quartz (25%), biotite (3.4%), amphibole (2.6%) and opaque minerals (1.8%). Chlorite (7.4%) and sericite (1%) alteration.

VG-04B LAT (N) 18° 29' 53.48" LONG (W) 64° 24' 26.71"

Virgin Gorda. Fine-grained enclave in hornblende tonalite (VG-04A). Plagioclase, quarts, amphibole, and opaque minerals. Secondary chlorite.

VG-05 LAT (N) 18° 25' 35" LONG (W) 64° 26' 42.61"

Virgin Gorda. South shore at the Baths facing Fallen Jerusalem.

Aphaeretic granodiorite with enclaves (variable). Plagioclase (46.6%), quartz (26%), potassium feldspar (13%), biotite (8.2%), amphibole (2.8%), and opaque minerals (>1%). Secondary chlorite alteration (2.8%).

VG-06 LAT (N) 18° 26' 29.07" LONG (W) 64° 26' 18.13"

Virgin Gorda. Construction site south of the bulk food market near the Baths.

Tonalite. Zoned plagioclase (59%), quartz (20.8%), potassium feldspar (6.4%), biotite (6.4%), amphibole (4%), and opaque minerals (1.8%). Secondary chlorite alteration (1.6%).

VG-07 LAT (N) 18° 25' 58.87" LONG (W) 64° 25' 30.03"

Virgin Gorda. Along road at Copper Mine Point.

Tonalite. Heavily fractured and altered. Plagioclase (54.8%), undulose quartz (24%), potassium feldspar (7.2%), biotite (2.8%), foliated amphibole (3.4%), and opaque minerals (1.4%). Secondary chlorite alteration (6.4%). Copper and molybdenum deposits.

VG-08 LAT (N) 18° 25' 57.50" LONG (W) 64° 25' 37.84"

Virgin Gorda. Along road cut near Copper Mine Point.

Tonalite with sparse enclaves (<15 cm). Plagioclase (49.6%), quartz (37.6%), potassium feldspar (3%), biotite (6.4%), foliated amphibole (1.4%), and opaque minerals (1%). Secondary chlorite alteration (<1%).Foliation dips shallowly eat-northeast 20-30°

VG-09A LAT (N) 18° 27' 43.81" LONG (W) 64° 26' 8.27"

Virgin Gorda. Western shoreline of Little Dix Bay.

Fine grained equigranular hornblende gabbro. Primary plagioclase, amphibole, pyroxene, olivine, and opaque minerals. Heavy chlorite alteration and iron oxidation.

VG-09B LAT (N) 18° 27' 43.81" LONG (W) 64° 26' 8.27"

Virgin Gorda. Western shoreline of Little Dix Bay.

Coarse grained hornblende gabbro. Plagioclase (>1cm), olivine, amphibole, and pyroxene. Olivine alteration with iddingsite rims. Pyroxene has lamellar twins.

VG-09C LAT (N) 18° 27' 43.81" LONG (W) 64° 26' 8.27"

Virgin Gorda. Western shoreline of Little Dix Bay.

Orbicular hornblende gabbro. Orbicules have plagioclase rich centers with radiating amphibole and pyroxene.

GD-10A LAT (N) 18° 28' 59.16" LONG (W) 64° 27' 42.19"

Great Dog at the Chimneys.

Enclave rich granodiorite/tonalite with epidotized fault surface along contact with mafic sheets. Primary plagioclase, amphibole, and opaque minerals. Secondary chlorite and sericite. Heavily weathered. Fine grained alteration products.

GD-10B LAT (N) 18° 28' 59.16" LONG (W) 64° 27' 42.19"

Great Dog at the Chimneys.

Mafic sheet in contact with enclave rich granodiorite/tonalite. Primary plagioclase, amphibole, and opaque minerals with secondary chlorite and sericite.

MC-11 LAT (N) 18° 27' 39.99" LONG (W) 64° 31' 37.38"

North shore of Marina Cay east of the dock.

Heavily weathered with primary plagioclase, amphibole, and opaque minerals with trace pyroxene. Secondary chlorite, sericite, and iron oxidation.

LC-12A LAT (N) 18° 27' 44.39" LONG (W) 64° 32' 38"

Little Camanoe. Along north shore.

North trending mafic dike cutting tonalite and small orthogonal mafic dike. Heavily altered with fine grained plagioclase and pyroxene. Secondary chlorite and sericite alteration.

LC-12B LAT (N) 18° 27' 44.39" LONG (W) 64° 32' 38"

Little Camanoe. Along north shore.

Tonalite. Plagioclase (46.2%), quartz (44.6%), potassium feldspar (6.2%), and opaque minerals (3%). Heavy sericite alteration.

LC-12C LAT (N) 18° 27' 44.39" LONG (W) 64° 32' 38"

Little Camanoe. Along north shore.

Small east-west trending mafic dike cutting tonalite and large orthogonal mafic dike. Heavily altered with fine grained plagioclase and pyroxene. Secondary sericite alteration.

PI-13A LAT (N) 18°19'55.89" LONG (W) 64°34'18.98"

Peter Island. Southwestern shoreline facing Norman Island.

Diorite. In contact with mafic a metamorphic sheets. Plagioclase (37.4%), quartz (1.3%). Trace olivine and opaque minerals. Heavily altered with sericite (49.6%), chlorite (9.2%), and trace calcite.

PI-13B LAT (N) 18°19'55.89" LONG (W) 64°34'18.98"

Peter Island. Southwestern shoreline facing Norman Island.

Basalt sheet in contact with diorite and metamorphic sheets. Primary plagioclase, amphibole, and pyroxene with secondary chlorite and sericite alteration.

PI-13C LAT (N) 18°19'55.89" LONG (W) 64°34'18.98"

Peter Island. Southwestern shoreline facing Norman Island.

Metamorphic sheet in contact with basalt and diorite sheets. Epidote, quartz veins, chlorite, and opaque minerals.

NI-14A LAT (N) 18° 19' 24.06" LONG (W) 64° 35' 55.82"

Norman Island. Eastern shoreline facing Peter Island.

Porphyritic quartz diorite with coarse grained granodiorite xenoliths. Plagioclase 74.8%, quartz (9.2%), potassium feldspar (3.6%), and amphibole (8.8%). Chlorite alteration (2.2%)

NI-14B LAT (N) 18° 19' 24.06" LONG (W) 64° 35' 55.82"

Norman Island. Eastern shoreline facing Peter Island.

Chilled margin of internal contacts of sheeted porphyritic quartz diorite. Ground mass (60.8%), plagioclase, quartz, and chlorite alteration.

CI-15A LAT (N) 18°23'16.39" LONG (W) 64°30'47.51"

Cooper Island. Western shore north of the dock.

Coarse grained tonalite. Plagioclase (49.2%), quartz (23%), amphibole (10.4%), and opaque minerals (1%). Secondary chlorite (14.2%) and sericite alteration.

CI-15B LAT (N) 18°23'16.39" LONG (W) 64°30'47.51"

Cooper Island. Western shore north of the dock.

Heavily altered volcaniclastic unit beneath tonalite. Secondary chlorite, sericite, and iron oxidation. Primary plagioclase, opaque minerals, and trace olivine.

VG-16A LAT (N) 18°29'29.00" LONG (W) 64°21'26.19"

Virgin Gorda. North sound west of Fat Virgin café.

Quartz diorite. Primary plagioclase (46.2%), quartz (37.4%), potassium feldspar (6.8%), amphibole (8.2%) and opaque minerals (1.4%). Minor secondary sericite and iron oxidation.

VG-16B LAT (N) 18°29'27.86" LONG (W) 64°21'16.78"

Virgin Gorda. South of Fat Virgin café on the south facing shoreline.

Tonalite. Primary plagioclase (41%), quartz (52%), and potassium feldspar (5.6%).

VG-17A LAT (N) 18°30'9.89" LONG (W) 64°20'55.60"

Virgin Gorda, past Bitter End and Saba rock on the north facing shoreline.

Tonalite. Primary plagioclase (50.2%), quartz (36.2%), potassium feldspar (1%), amphibole (5.4%), and trace opaque minerals. Secondary chlorite (6.2%) and sericite alteration.

VG-17B LAT (N) 18°30'9.89" LONG (W) 64°20'55.60"

Virgin Gorda, past Bitter End and Saba rock on the north facing shoreline.

Volcaniclast screen. Plagioclase, pyroxene, amphibole, and opaque minerals. Iron staining and sericite alteration.

VG-18 LAT (N) 18° 29' 22.09" LONG (W) 64° 22' 12.43"

Virgin Gorda. Western side of bay in North sound along the shoreline.

Tonalite. Primary plagioclase (48.6%) and quartz (18.6%). Heavy chlorite (25.6%) and sericite alteration.

VG-19 LAT (N) 18° 29' 22.09" LONG (W) 64° 22' 12.43"

Virgin Gorda. Western side of bay in North sound along the shoreline.

Heavily altered plagioclase, plagioclase, quartz, amphibole, and opaque minerals. Secondary sericite and minor chlorite alteration

VG-20 LAT (N) 18° 29' 22.09" LONG (W) 64° 22' 12.43"

Virgin Gorda. Eastern side of bay in North Sound along the shoreline.

Heavily altered plagioclase, amphibole, and quartz. Secondary sericite, chlorite, and oxide alteration.

VG-22 LAT (N) 18° 27' 21.96" LONG (W) 64° 25' 45.26"

Virgin Gorda. The Valley, just north of Olde Yard Village.

Enclave rich tonalite. Plagioclase (45.8%), 28.2 (%), potassium feldspar (4%), biotite (8.2%), amphibole (7.8%) and opaque minerals (2.4%). Secondary chlorite (3.6%) and trace epidote.

VG-23A LAT (N) 18° 27' 59.36" LONG (W) 64° 24' 54.29"

Virgin Gorda. Along Pond Bay road cut.

Fine grained mafic unit north of VG-23B. Primary plagioclase, amphibole, and opaque minerals. Secondary chlorite and sericite alteration.

VG-23B LAT (N) 18° 27' 59.36" LONG (W) 64° 24' 54.29"

Virgin Gorda, Along Pond Bay road cut.

Fine grained mafic unit south of VG-23A. Lower color index than VG-23A. Heavily weathered primary plagioclase, amphibole, and opaque minerals. Secondary chlorite and sericite.

VG-24 LAT (N) 18° 29' 6.07" LONG (W) 64° 24' 49.64"

Virgin Gorda, at Mountain Trunk Bay near steeply dipping fault zone (2.5 m).

Tonalite. Fine grained plagioclase (54.2%), quartz (15.4%), amphibole (18%) and opaque minerals (3%). Secondary chlorite (9.4%) and sericite alteration.

TO-25 LAT (N) 18°26'44.05" LONG (W) 64°33'19.62"

Tortola. Along road cut just before bridge to Beef Island

Quartz diorite. Plagioclase (51.6%), quartz (12%), amphibole (23.8%), and opaque minerals (2.8%). Secondary chlorite (9.8%) and sericite alteration.

BI-26 LAT (N) 18°26'34.96" LONG (W) 64°32'35.74"

Beef Island. Road cut past bridge from Tortola next to the airport.

Tonalite. Plagioclase (45.8%), quartz (30.4%), potassium feldspar (3%), amphibole (9.6%), biotite (8.8%), and trace opaque minerals. Secondary chlorite (2%) and sericite alteration.

REFERENCES

Albarède, F., 1998, The growth of continental crust, Tectonophysics, v. 296, p. 1-14.

Annen, C., Blundy, J. D., and Sparks, S. J., 2006, The genesis of intermediate and silicic magmas in deep crustal hot zones: Journal of Petrology, v. 47, no. 3, p. 505-539.

Barth, M. G., McDonough, W. F., and Rudnick, R. L., 2000, Tracking the budget of Nb and Ta in the continental crust: Chemical Geology, v. 165, p. 197-213.

Beard, J. S., and Barker, F., 1989, Petrology and tectonic significance of gabbros, tonalites, shoshonites, and anorthosites in a Late Paleozoic arc-root complex in the Wrangellia terrane, Southern Alaska: Journal of Geology, v. 97, p. 667-683.

Beard, J. S., and Day, H. W., 1988, Petrology and emplacement of reversely zoned gabbro-diorite plutons in the Smartville Complex, Northern California: Journal of Petrology, v. 29, no. 5, p. 965-995.

Beard, J. S., 1995, Experimental, geological, and geochemical constraints on the origins of low-K silicic magmas in oceanic arcs: Journal of Geophysical Research, v. 100, no. B8, p. 15,593-15,600.

Behn, M. D., and Kelemen, P. B., 2006, Stability of arc lower crust: Insights from the Talkeetna arc section, south central Alaska, and the seismic structure of modern arcs: Journal of Geophysical Research, v. 111, B11207, doi:10.1029/2006JB004327.

Bindeman, I., 2008, Oxygen isotopes in Mantle and crustal magmas as revealed by single crystal analysis: Reveiws in Mineralogy and Geochemistry, v. 69, p. 445-478.

Bowen, N. L., 1928, The evolution of the igneous rocks: Princeton, New Jersey, Princeton University Press, 334 p.

Brophy, J. G., 2008, A study of rare earth element (REE)-SiO_2 variations in felsic liquids generated by basalt fractionation and amphibolite melting: a potential test for discriminating between the two different processes: Contributions to Mineralogy and Petrology, v. 156, p. 337-357, doi:10.1007/s00410-008-0289-x.

Byrne, D. B., Suarez, G., and McCann, W. R., 1985, Muertos Trough subduction-Microplate tectonics in the northern Caribbean: Nature, v. 317, p. 420-421.

Case, J. E., MacDonald, W. D., and Fox, P. J., 1990, Caribbean crustal provinces; seismic and gravity evidence, *in* Dengo, G., and Case, J. E., eds., The Caribbean region: Boulder, Colorado, Geological Society of America, Geology of North America, v. H, p. 15-36.

Condie, K. C., 1990, Growth and accretion of continental crust: Inferences based on Laurentia: Chemical Geology, v. 83, p. 183-194.

Condie, K. C., and Chomiak, B., 1996, Continental accretion: contrasting Mesozoic and Early Proterozoic tectonic regimes in North America: Tectonophysics, v. 265, p, 101-126.

Cox, D. P., Marvin, R. F., M'Gonigle, J. W., McIntyre, D. H., and Rogers, C. L., 1977, Potassium-argon geochronology of metamorphic, igneous, and hydrothermal events in Puerto Rico and the Virgin Islands: U.S. Geological Survey Journal of Research, v. 5, p. 689-703.

Davidson, J. P., Turner, S., Handley, H., Macpherson, C., and Dosseto, A., 2007, Amphibole "sponge" in arc crust?: Geology, v. 35, no. 9, p. 787-790, doi: 10.1130/G23637A.1.

Davidson, J. P., 1987, Crustal contamination versus subduction zone enrichment: examples from the Lesser Antilles and implications for mantle source compositions of island arc volcanic rocks: Geochimica et Cosmochimica Acta, v. 51, p. 2185-2198.

Davidson, J. P., 1986, Isotopic and trace element constraints on the petrogenesis of subduction-related lavas from Martinique, Lesser Antilles: Journal of Geophysical Research, v. 91, p. 5943-5962.

DeBari, S. M., and Sleep, N. M., 1991, High-Mg, low-Al bulk composition of the Talkeetna island arc, Alaska: implications for primary magmas and the nature of arc crust: Geological Society of America Bulletin, v. 103, p. 37-47.

Devine, C. D., 1969, The stability constants of some carboxylate complexes of the trivalent lanthons [Ph.D. thesis]: Iowa State University, 163 p.

Draper, G., Guitierrez, G., and Lewis, J. F., 1996, Thrust emplacement of the Hispaniola peridotite belt; orogenic expression of the mid-Cretaceous Caribbean arc polarity reversal?: Geology, v. 24, no. 12, p. 1143–1146.

Drummond, M. S., Defant, M. J., and Kepezhinska, P. K., 1996, Petrogenesis of slab-derived trondhjemite-tonalite-dacite/adakite magmas *in* Brown, M., Candela, P.A., Peck, D. L., Stephens, W. E., Walker, R. J., Zen, E-an., eds., The third Hutton symposium on the origin of granites and related rocks: Boulder, Colorado, Geological Society of America Special Paper, v. 315, p. 205-215.

Donnelly, T. W., and Rogers, J. J. W., 1980, Igneous series in island areas; the northeastern Caribbean compared with worldwide island-arc assemblages: Bulletin Volcanologique, v. 43, no. 2, p. 347-382.

Donnelly, T. W., and Rogers, J. J. W., 1978, The distribution of igneous rock suites throughout the Caribbean: Geologie en Mijnbouw, v. 57, p. 151-162.

Donnelly, T. W., Beets, D., Carr, M. J., Jackson, T., Klaver, G., Lewis, J., Maury, R., Schellekens, H., Smith, A L., Wadge, G., and Westercamp, D., 1990, History and tectonic setting of Caribbean magmatism, *in* Dengo, G., and Case, J. E., eds., The Caribbean region: Boulder, Colorado, Geological Society of America, Geology of North America, v. H, p. 339-374.

Frost, C. D., Schellekens, J. H., and Smith, A. L., 1998, Nd, Sr, and Pb isotopic characterization of Cretaceous and Paleogene volcanic and plutonic island arc rocks from Puerto Rico, *in* Lidiak, E. G., and Larue., D. K., eds., Tectonics and Geochemistry of the Northeastern Caribbean: Boulder, Colorado, Geological Society of America Special Paper 322, p. 123-132.

Gill, J. B., and Stork, A. L., 1979, Miocene low-K dacites and trondhjemites of Fiji, *in* Barker, F., ed., Trondhjemites, Dacites, and Related Rocks: New York, Elsevier, p. 629-649.

Greene, A. R., DeBari, S. M., Kelemen, P. B., Blusztajn, J., and Clift, P. D., 2006, A detailed geochemical study of island arc crust: the Talkeetna Arc section, South-Central Alaska: Journal of Petrology, v. 47, no. 6, p. 1051-1093, doi:10.1093/petrology/egl002.

Hastie, A. R., 2009, Is the Cretaceous primitive island arc series in the circum-Caribbean region geochemically analogous to the modern island arc tholeiite series?: Geological Society, London, Special Publications, v. 328, p. 399-409, doi:10.1144/SP328.16.

Hamilton, W., 1981, Crustal evolution by arc magmatism: Philosophical transactions of the Royal Society of London, v. 301, no. 1461, p. 279-291.

Helsley, C. E., 1971, Summary of the geology of the British Virgin Islands, *in* Mattson, P. H., ed., Transactions Fifth Caribbean Geological Conference, St. Thomas, U.S. Virgin Islands, 1968: New York, Queens College Press, p. 69-76.

Helsley, C. E., 1960, Geology of the British Virgin Islands: Princeton, N.J., Princeton University, [Ph.D. thesis], 219 p.

Hildreth, W., and Moorbath, S., 1988, Crustal contributions to arc magmatism in the Andes of Central Chile: Contributions to Mineralogy and Petrology, v. 98, p. 455-489.

Jagoutz, O. E., Burg, J. –P., Hussain, S., Dawood, H., Pettke, T., Iizuka, T., and Maruyama, S., 2009, Construction of the granitoid crust of an island arc part I: geochronological and geochemical constraints from the plutonic Kohistan (NW Pakistan): Contrib. Mineral. Petrol., DOI:10.1007/s00410-009-0408-3.

Jagoutz, O., Müntener, O., Burg, J. –P., Ulmer, P., and Jagoutz, E., 2006, Lower continental crust formation through focused flow in km-scale melt conduits: The zoned ultramafic bodies of the Chilas Complex in the Kohistan island arc (NW Pakistan): Earth and Planetary Science Letters, v. 242, p. 320-342.

James, K. H., 2009, Evolution of middle America and the *in situ* Caribbean Plate model: *in* James, K. H., Lorente, M. A., and Pindell, J. L., eds., The Origin and evolution of the Caribbean plate: Geological Society, London, Special Publications, v. 328, p. 127-138.

Jansma, P. E., Mattioli, G. S., Lopez, A., DeMets, C., Dixon, T., Mann, P., Calais, E., 2000, Neotectonics of Puerto Rico and the Virgin Islands, northeastern Caribbean from GPS geodesy: Tectonics, v. 19, no. 6, p. 1021-1037.

Jochum, K. P., Pfänder, J., Snow, J. E., Hofmann, A. W., 1997, Nb/Ta in mantle and crust. EOS, Transactions, Am. Geophys. Union, v. 78, no. 46, Suppl., p. 805.

Jolly, W. T., Lidiak, E. G., and Dickin, A. P., 2008, The case for persistent southwest-dipping Cretaceous convergence in the northeast Antilles: Geochemistry, melting models, and tectonic implications: Geological Society of America Bulletin, v. 120, no. 7/8, p. 1036-1052, doi:10.1029/2006GC001335.

Jolly, W. T., Lidiak, E. G., Dickin, A. P., and Wu, T. -W., 1998a, Geochemical diversity of Mesozoic island arc tectonic blocks in eastern Puerto Rico, *in* Lidiak, E. G., and Larue., D. K., eds., Tectonics and Geochemistry of the Northeastern Caribbean: Boulder, Colorado, Geological Society of America Special Paper 322, p. 67-98.

Jolly, W. T., Lidiak, E. G., Schellekens, J. H., and Santos, H., 1998b, Volcanism, tectonics, and stratigraphic correlations in Puerto Rico, *in* Lidiak, E. G., and Larue., D. K., eds., Tectonics and Geochemistry of the Northeastern Caribbean: Boulder, Colorado, Geological Society of America Special Paper 322, p. 1-34.

Joyce, J., 1991, Blueschist metamorphism and deformation on the Samana Peninsula-A record of subduction and collision in the Greater Antilles, *in* Mann, P., Draper, G., and Lewis J. F., eds., Geologic and tectonic development of the North America-Caribbean plate boundary in Hispaniola: Geological Society of America Special Paper 262, p. 47-76.

Kemp, A. I. S., Hawkesworth, C. J., Foster, G. L., Paterson, B. A., Woodhead, J. D., Hergt, J. M., Gray, C. M., and Whitehouse, M. J., 2007, Magmatic and crustal differentiation history of granitic rocks from Hf-O isotopes in zircon: Science, v. 315, p. 980-983.

Kerr, A. C., Iturralde-Vinent, M. A., Saunders, A. D., Babbs, T. L., and Tarney, J., 1999, New plate tectonic model of the Caribbean: Implications from a geochemical reconnaissance of Cuban Mesozoic volcanic rocks, Geological Society of America Bulletin, v. 111, no. 11, p. 000-000.

Kesler, S. E., and Sutter, J. F., 1979, Compositional evolution of intrusive rocks in the eastern Greater Antilles island arc: Geology, v. 7, p. 197-200.

Khan, M. A., Jan, M. Q., and Weaver, B. L., 1993: Evolution of the lower arc crust in Kohistan, N. Pakistan: temporal arc magmatism through early, mature and intra-arc rift stages, *in* Treloar, P. J., and Searle, M. P., eds., Himalayan Tectonics: London, Geological Society Special Paper, v. 74, p. 123-138.

Krogh, T. E., 1973, A low-contamination method for hydrothermal decomposition of zircon and extraction of U and Pb for isotopic age determinations: Geochimica et Cosmochimica Acta, v. 37, no. 3, p. 485-494.

Lee, C. –T. A., Cheng, X., and Horodyskyj, U., 2006, The development and refinement of continental arcs by primary basaltic magmatism, garnet pyroxenite accumulation, basaltic recharge and delamination: insights from the Sierra Nevada, California: Contrib. Mineral Petrol, v. 151, p. 222-242.

Lewis, J. F., and Draper, G., 1990, Geology and tectonic evolution of the northeastern Caribbean margin: *in* Dengo, G., and Case, J. E., eds., The Caribbean region: Boulder, Colorado, Geological Society of America, Geology of North America, v. H, p. 77-140.

Lidiak, E. G., and Jolly, W. T., 1998, Geochemistry of intrusive igneous rocks, St. Croix, U.S. Virgin Islands, *in* Lidiak, E. G., and Larue., D. K., eds., Tectonics and Geochemistry of the Northeastern Caribbean: Boulder, Colorado, Geological Society of America Special Paper 322, p. 133-153.

Lidiak, E. G., and Jolly, W. T., 1996, Circum-Caribbean granitoids: Characteristics and origin: International Geology Review, v. 38, p. 1098–1133.

Longshore, J. D., 1965, Chemical and mineralogical variations in the Virgin Islands batholith and its associated wall rocks [Ph.D. thesis]: Houston, Rice University, 94 p.

Ludwig, K. R., 2003, Using Isoplot/Ex, Version 3, A geochronological toolkit for Microsoft Excel: Berkeley Geochronology Ctr. Spec. Pub. 4

Ludwig, K. R., 1990, ISOPLOT: A plotting and regression program for radiogenic isotope data, for IBM-PC compatible computers, version 2.02, U.S. Geological Survey Open-File Report 88-557, 44 p.

Ludwig, K. R., 1989, PbDAT for MSDOS: A computer program for IBM-PC compatibles for processing raw Pb-U-Th isotope data, version 1.06, U.S. Geological Survey Open-File Report 88-542, 40 p.

Mattinson, J. M., 2005, Zircon U/Pb chemical abrasion (CA-TIMS) method; combined annealing and multi-step partial dissolution analysis for improved precision and accuracy of zircon ages: Chemical Geology, v. 220, no. 1-2, p. 47-66.

Mundil, R., Ludwig, K. R., Metcalfe, I., and Renne, P. R., 2004, Age and timing of the Permian mass extinctions; U/Pb dating of closed-system zircons: Science, v. 305, p. 1760-1763.

Parrish, R. R., and Krogh, T. E., 1987, Synthesis and purification of 205Pb for U-Pb geochronology: Chemical Geology; Isotope Geosciences Section, v. 66, no. 1-2, p. 103-110.

Petford, N., Cruden, A. R., McCaffrey, K. J. W., and Vigneresse, J. L., 2000, Granite magma formation, transport and emplacement in the Earth's crust: Nature, v. 408, no. 6813, p. 669-673.

Peate, D. W., Pearce, J. A., Hawkesworth, C. J., Colley, H., Edwards, C. M. H., and Hirose, K., 1997, Geochemical variation in Vanuatu Arc lavas: The role of subducted material and variable mantle wedge composition: Journal of Petrology, v. 38, p. 1331-1358.

Pindell, J. L., and Barrett, S. F., 1990, Geological evolution of the Caribbean region: a plate tectonic perspective, *in* Dengo, G. and Case, J. E., eds., The Caribbean region: Boulder, Colorado, Geological Society of America, The Geology of North America, v. H, p. 405-432.

Pindell, J. L., and Kennan, L., 2009, Tectonic evolution of the Gulf of Mexico, Caribbean and northern South America in the mantle reference frame: an update: *in* James, K. H., Lorente, M. A., and Pindell, J. L., eds., The Origin and evolution of the Caribbean plate: Geological Society, London, Special Publications, v. 328, p. 1-55.

Pindell, J. L., Kennan, L., Stanek, K.P., Maresch, W.V., and Draper, G., 2006, Foundation of Gulf of Mexico and Caribbean evolution: eight controversies resolved: Geologica Acta, v. 4, no. 1-2, p. 303-341.

Pitcher, W., 1997, The nature and origin of Granite: London, Chapman & Hall, 321 p.

Rapp, P. R., Watson, E. B., and Miller, C. F., 1991, Partial melting of amphibolite/eclogite and the origin of Achaean trondhjemites and tonalites: Precambrian Research, v. 51, p. 1-25.

Reid, J. A., Plumley, P. W., and Schellekens, J. H., 1991, Paleomagnetic evidence for Late Miocene counter-clockwise rotation of north-coast carbonate sequence, Puerto Rico: Geophysical Research Letters, v. 18, p. 565-568.

Rosencrantz, E., and Sclater, J. G., 1987, Depth magnetic anomalies and spreading in the Cayman Trough: EOS (Transactions, American Geophysical Union), v. 68, p. 405-406.

Rubatto, D., and Hermann, J., 2007,Experimental zircon/melt and zircon/garnet trace element partitioning and implications for the geochronology of crustal rocks: Chemical Geology, v. 241, p. 38-61.

Rudnick, R. L., 1995, Making continental crust: Nature, v. 378, p. 571-578.

Rudnick, R. L., 1992, Restites, Eu anomalies, and the lower continental crust: Geochimica and Cosmochimica Acta, v. 56, p. 963-970.

Rudnick, R. L., and Fountain, D. M., 1995, Nature and composition of the continental crust: a lower crustal perspective: Rev. Geophys., v. 33, p. 267-309.

Smith, A. L., Schellekens, J. H., and Muriel Díaz, A. -L., 1998, Batholiths as markers of tectonic change in the northeastern Caribbean, *in* Lidiak, E. G., and Larue., D. K., eds., Tectonics and Geochemistry of the Northeastern Caribbean: Boulder, Colorado, Geological Society of America Special Paper 322, p. 99-122.

Smithies, R. H., Champion, D. C., and Cassidy, K. F., 2003, Formation of Earth's early Achaean continental crust: Precambrian Research, v. 127, p. 89-101.

Steiger, R. H., and Jäger, E., 1977, Subcommission on Geochronology; convention on the use of decay constants in geochronology and cosmochronology, *in* 25th International geological congress, Geological time scale symposium, Sydney, Australia, p. 67-71.

Stork, A. L., 1984, Silicic magmatism in an island Arc, Fiji, Southwest Pacific; implications for continental growth [Ph.D. thesis]: University of California at Santa Cruz.

Sun, S. S., and McDonough, W. F., 1989, Chemical and isotopic systematics of oceanic basalts; implications for mantle composition and processes, *in* Saunders, A. D., and Norry, M. J., eds., Magmatism in the ocean basins. Geological Society of London Special Publications, v. 42, pp 313–345.

Tanaka, T., Togashi, S., Kamioka, H., Amakawa, H., Kagami, H., Hamamoto, T., Yuhara, M., Orihashi, Y., Yoneda, S., Shimizu, H., Kunimaru, T., Takahashi, K., Yanagi, T., Nakano, T., Fujimaki, H., Shinjo, R., Ashara, Y., Tanimizu, M., and Dragusanu, C., 2000, JNdi-1: a neodymium isotopic reference in consistency with LaJolla neodymium: Chemical Geology, v. 168, p. 279-281.

Taylor, S. R., 1966, The origin and growth of continents: Tectonophysics, v. 4, no. 1, p. 17-34.

Taylor, S. R., and McLennan, S. M., 1995, The geochemical evolution of the continental crust: Review of Geophysics, v. 33, p. 241-265.

Taylor, S. R., and McLennan, S. M., 1985, The continental crust: its composition and evolution, Blackwell, Oxford, 312 p.

Valley, J. W., Lackey, J. S., Cavosie, A. J., Clechenko, C. C., Spicuzza, M. J., Basei, M. A. S., Bindeman, I. N., Ferreira, V. P., Sial, A. N., King, E. M., Peck, W. H., Sinha, A. K., and Wei, C. S., 2005, 4.4 billion years of crustal maturation: oxygen isotope ratios of magmatic zircon: Contrib. Mineral. Petrol., v. 150, p. 561-580.

Vila, J. –M., Andreieff, P., Bellon, H., and Mascle, A., 1986, Tectonique de collage le long d'un accident décrochant, ante oligocéne, est-ouest, dans les Iles Vierges septentrionales (Antilles): Comptes Rendus Académie des Sciences, Paris, Tome 302, série II, no. 3, p. 141-144.

von Huene, R., and Scholl, D. W., 1991, Observations at convergent margins concerning sediment subduction, subduction erosion, and the growth of continental crust: Reviews of Geophysics, v. 29, no. 3, p. 279-316.

Weaver, B. L., and Tarney, J., 1984, Empirical approach to estimating the composition of the continental crust: Nature, v. 310, p. 575-577.

Wedepohl, K. H., 1995, The composition of the continental crust: Geochimica et Cosmochimica Acta, v. 59, no. 7, p. 1217-1232.

White, W. M., and Dupré, B., 1986, Sediment subduction and magma genesis in the Lesser Antilles: isotopic and trace element constraints: Journal of Geophysical Research, v. 91, p.5927-5941.

White, W. M., Dupré, B., and Vidal, P., 1985, Isotope and trace element geochemistry of sediments from the Barbados Ridge-Demerara Plain region, Atlantic Ocean: Geochimica et Cosmochimica Acta, v. 49, p. 1875-1886.

White, W. M., and Dupré, B., 1986, Sediment subduction and magma genesis in the Lesser Antilles: isotopic and trace element constraints: Journal of Geophysical Research, v. 91, p.5927-5941.

White, W. M., Dupré, B., and Vidal, P., 1985, Isotope and trace element geochemistry of sediments from the Barbados Ridge-Demerara Plain region, Atlantic Ocean: Geochimica et Cosmochimica Acta, v. 49, p. 1875-1886.